Cellular/Molecular

PGE2 Potentiates Orai1-Mediated Calcium Entry Contributing to Peripheral Sensitization

Dongyu Wei,[1] Hareram Birla,[2] Yannong Dou,[1] Yixiao Mei,[1] Xiaodong Huo,[2] Victoria Whitehead,[2] Patrick Osei-Owusu,[2] Stefan Feske,[3] Giovanna Patafio,[2] Yuanxiang Tao,[2] and Huijuan Hu[1,2]

[1]Department of Pharmacology and Physiology, Drexel University College of Medicine, Philadelphia, Pennsylvania 19102, [2]Department of Anesthesiology, Rutgers New Jersey Medical School Newark, Newark, New Jersey 07103, and [3]Department of Pathology, NYU Grossman School of Medicine, New York, New York 10016

Peripheral sensitization is one of the primary mechanisms underlying the pathogenesis of chronic pain. However, candidate molecules involved in peripheral sensitization remain incompletely understood. We have shown that store-operated calcium channels (SOCs) are expressed in the dorsal root ganglion (DRG) neurons. Whether SOCs contribute to peripheral sensitization associated with chronic inflammatory pain is elusive. Here we report that global or conditional deletion of Orai1 attenuates Complete Freund's adjuvant (CFA)-induced pain hypersensitivity in both male and female mice. To further establish the role of Orai1 in inflammatory pain, we performed calcium imaging and patch-clamp recordings in wild-type (WT) and Orai1 knockout (KO) DRG neurons. We found that SOC function was significantly enhanced in WT but not in Orai1 KO DRG neurons from CFA- and carrageenan-injected mice. Interestingly, the Orai1 protein level in L3/4 DRGs was not altered under inflammatory conditions. To understand how Orai1 is modulated under inflammatory pain conditions, prostaglandin E2 (PGE2) was used to sensitize DRG neurons. PGE2-induced increase in neuronal excitability and pain hypersensitivity was significantly reduced in Orai1 KO mice. PGE2-induced potentiation of SOC entry (SOCE) was observed in WT, but not in Orai1 KO DRG neurons. This effect was attenuated by a PGE2 receptor 1 (EP1) antagonist and mimicked by an EP1 agonist. Inhibition of Gq/11, PKC, or ERK abolished PGE2-induced SOCE increase, indicating PGE2-induced SOCE enhancement is mediated by EP1-mediated downstream cascade. These findings demonstrate that Orai1 plays an important role in peripheral sensitization. Our study also provides new insight into molecular mechanisms underlying PGE2-induced modulation of inflammatory pain.

Key words: **dorsal root ganglion neuron; EP1; Orai1; PGE2; store-operated calcium channels**

Significance Statement

Store-operated calcium channel (SOC) Orai1 is expressed and functional in dorsal root ganglion (DRG) neurons. Whether Orai1 contributes to peripheral sensitization is unclear. The present study demonstrates that Orai1-mediated SOC function is enhanced in DRG neurons under inflammatory conditions. Global and conditional deletion of Orai1 attenuates complete Freund's adjuvant (CFA)-induced pain hypersensitivity. We also demonstrate that prostaglandin E2 (PGE2) potentiates SOC function in DRG neurons through EP1-mediated signaling pathway. Importantly, we have found that Orai1 deficiency diminishes PGE2-induced SOC function increase and reduces PGE2-induced increase in neuronal excitability and pain hypersensitivity. These findings suggest that Orai1 plays an important role in peripheral sensitization associated with inflammatory pain. Our study reveals a novel mechanism underlying PGE2/EP1-induced peripheral sensitization. Orai1 may serve as a potential target for pathological pain.

Received Feb. 22, 2023; revised Aug. 9, 2023; accepted Aug. 29, 2023.

Author contributions: D.W., H.B., Y.D., and H.H. designed research; D.W., H.B., Y.D., Y.M., and X.H. performed research; D.W., H.B., Y.D., Y.M., X.H., V.W., G.P., and H.H. analyzed data; D.W. wrote the first draft of the paper; D.W., H.B., Y.D., Y.M., X.H., V.W., P.O., S.F., G.P., Y.T., and H.H. edited the paper; P.O., S.F., and H.H. wrote the paper.

The authors thank Professor Kendall Blumer of Washington University School of Medicine in St. Louis, MO, for kindly providing FR900359. This work was supported by NINDS Grants R01NS087033, R01NS128403, and R01R01NS117484.

The authors declare no competing financial interests.

Correspondence should be addressed to Huijuan Hu at hh480@njms.rutgers.edu.

https://doi.org/10.1523/JNEUROSCI.0329-23.2023

Introduction

Chronic inflammatory pain can be caused by peripheral tissue inflammation, which is characterized as hypersensitivity to noxious and non-noxious stimuli (hyperalgesia and allodynia) and spontaneous pain (Scholz and Woolf, 2002). One of the primary mechanisms contributing to chronic inflammatory pain is peripheral sensitization, which leads to increased excitability of nociceptive dorsal root ganglion (DRG) neurons innervating the inflamed tissues (Woolf and Ma, 2007). Prostaglandin E2

(PGE2), a major inflammatory mediator, plays an important role in peripheral sensitization associated with inflammatory pain as well as spinal nerve-induced neuropathic pain. PGE2 is released at the site of tissue damage or nerve injury (Guay et al., 2004; Ma et al., 2010; Gao et al., 2013) and acts on four receptor subtypes (EP1–EP4), all G-protein-coupled receptors (GPCRs) to exert its various actions, including pyrexia, pain sensation, and inflammation (Kawabata, 2011; Brudvik and Tasken, 2012; Das, 2021; Shionoya et al., 2022). It is well established that EP1 couples to the Gq/11 (Gq protein alpha subunit 11) signaling pathway, EP2 and EP4 associate with Gs to upregulate cAMP signaling, while EP3, acting via the Gi/o-signaling pathway, inhibits cAMP generation (Alfranca et al., 2006).

Among the four PGE2 receptors, EP1 and EP4 play a major role in inflammatory pain (Lin et al., 2006; Clark et al., 2008; Ma et al., 2010; Cruz Duarte et al., 2012). EP1 is expressed in DRG neurons but not in the spinal cord (Nakayama et al., 2004). In agreement with this finding, a previous study showed that peripheral but not central EP1 receptors play a major role in PGE2-induced pain sensitization (Johansson et al., 2011). Inhibition or deletion of EP1 reduces nociception, PGE2-induced thermal hyperalgesia, and inflammatory nociceptive responses (Minami et al., 2001; Stock et al., 2001; Nakayama et al., 2004; Moriyama et al., 2005; Johansson et al., 2011). EP2 is widely expressed in many cell types of the body and is involved in inflammation-related diseases, including neurodegenerative diseases, rheumatoid arthritis, and tumor angiogenesis (Ganesh et al., 2014; O'Callaghan and Houston, 2015; Shu et al., 2017). And it has been reported to contribute to PGE2-induced hyperalgesia via a central mechanism (Reinold et al., 2005). Blocking or deleting EP4 in peripheral nerves significantly attenuates rheumatoid arthritis and osteoarthritis (Caselli et al., 2018; Zhu et al., 2020). In contrast to other EP receptors, activation of EP3 reduces hyperalgesia and produces profound analgesia in rats with acute inflammation (Bar et al., 2004; Natura et al., 2013). Mechanistically, PGE2 has been shown to enhance the function of acid-sensing ion channels (ASICs) and transient receptor potential vanilloid 1 (TRPV1) in DRG neurons through EP1 and EP4 receptors (Lin et al., 2006; Ma et al., 2017; Zhou et al., 2019). Activation of the EP2/EP4 protein kinase A pathway increases tetrodotoxin-resistant (TTX-R) sodium currents (Matsumoto et al., 2005), which is attenuated by EP3 agonist (Konig et al., 2022), suggesting that PGE2 sensitizes nociceptors by stimulating multiple targets, including ion channels via different EP receptor subtypes and their signaling pathways.

Store-operated calcium channels (SOCs) are highly calcium-selective cation channels composed of three pore-forming Orai proteins located in the plasma membrane, Orai1/2/3, also known as Ca^{2+} release-activated Ca^{2+} channels (CRAC channels), and two endoplasmic reticulum (ER) membrane-located Ca^{2+} sensors, stromal interaction molecules (STIM) 1, and STIM2 (Lewis, 2007). SOCs can be activated by depletion or reduction of Ca^{2+} from intracellular stores (Putney, 2010). SOC entry (SOCE) is an essential process used to replenish intracellular Ca^{2+} stores (Putney, 2011), mediating many significant biological processes, including endothelial proliferation, skeletal muscle contractility, smooth muscle migration and proliferation, brain development, and immune function (Targos et al., 2005; Prakriya and Lewis, 2015). SOCE is a primary mechanism for Ca^{2+} influx into nonexcitable cells, which has been extensively investigated in immune cells (Targos et al., 2005; Hogan et al., 2010). Although the expression and function of SOCs have been reported in the nervous system (NS) including neurons and glia (Samtleben et al., 2015; Zhang and Hu, 2020; Lim et al., 2021), the role of SOCs in NS has not been well established. We have demonstrated that YM-58483, a potent SOC inhibitor, attenuates complete Freund's adjuvant (CFA)-, collagen-, and spared nerve injury-induced chronic pain in mice (Gao et al., 2013, 2015). A report from another group has further confirmed that YM-58483 alleviates neuropathic pain (Qi et al., 2016). These studies suggest that SOCs play a crucial role in chronic pain. However, the mechanism by which SOCs are involved in pain processing remains unclear. We also reported that Orai1 is expressed and functional in DRG neurons (Wei et al., 2017); however, whether Orai1 contributes to peripheral sensitization remains to be established.

Our previous study has revealed that Orai1 is an important component of SOCs in DRG neurons, (Wei et al., 2017). In this study, we show that SOCE is increased under inflammatory conditions, Orai1 deficiency attenuates CFA-induced pain hypersensitivity, and Orai1 is responsible for inflammation-induced SOCE increase in DRG neurons. We also demonstrate that inflammatory mediator, PGE2, potentiates SOCE in DRG neurons, and this effect is mediated through the EP1 and its downstream pathway. More importantly, we have found that Orai1 deficiency diminishes PGE2-induced increase in SOCE in DRG neurons and reduces PGE2-induced increase in neuronal excitability and pain hypersensitivity. These findings suggest that Orai1 plays an important role in peripheral sensitization associated with inflammatory pain. Our study reveals a novel mechanism underlying PGE2/EP1-induced peripheral sensitization.

Materials and Methods

Animals. All experiments were performed in accordance with the guidelines of the National Institutes of Health, the Committee for Research and Ethical Issues of IASP, and were approved by the Animal Care and Use Committee of Rutgers New Jersey Medical School (PROTO201800156) and Drexel University College of Medicine (PROTOCOL20516). Pregnant CD1 and C57BL/6 mice were purchased from Charles River and individually housed in standard cages on a 12 h light/dark cycle. CD1 and C57BL/6 mice were used for cell cultures, immunostaining, real-time PCR, Western blot experiments, and behavior studies. Orai1 mutant mice were generated by inserting a β-Geo cassette into the first intron of the Orai1 gene (Vig et al., 2008). These mice were originally purchased from Mutant Mouse Regional Resource Centers (MMRRC) and backcrossed into the CD1 genetic background for more than eight generations. $Orai1^{fl/fl}$ mice were received from Dr. S.F. at New York University Grossman School of Medicine and generated as described previously (Somasundaram et al., 2014; Kaufmann et al., 2016). Advillin-Cre mice were originally purchased from the Jackson Laboratory. For behavioral experiments, adult (8–10 weeks) male and female mice were used.

Genotyping. Mice were genotyped by PCR of DNA extracted from tail clippings. For genotyping of Orai1 mutant mice, the following primers were used for β-Geo: 5′-CAAATGGCGATTACCGTTGA (F), 5′-TGCCCAGTCATAGCCGAATA (R); for Tcrd: 5′-CAAATGTTGCTT GTCTGGTG (F), 5′-GTCAGTCGAGTGCACAGTTT (R). Copy number analysis using a TaqMan Genotyping Master Mix kit (Applied Biosystems) was used to further determine the genotypes following the manufacturer's instructions as described in our recent study (Dou et al., 2018). For Orai1 flox mice, 5′-GAAATGGCTCGGGGACAA AACACTA (F), 5′-GCCATTTCTGGTCTTCT-GGAGACTCTG (R). For Cre-recombinase, 5′-CATTTGGGCCAGCTAAACAT (F), 5′-TGC ATGATCTCCGGTATTGA (R).

Cell culture. Primary cultures of mouse DRG neurons were prepared as described previously (Wei et al., 2017). Briefly, DRGs were removed from adult mice (6–8 weeks old) and collected in cold (4°C) Hanks

balance salt solution (HBSS; Corning cellgro) containing 10 mM HEPES (Sigma Aldrich). Ganglia were incubated for 30 min at 37°C in HBSS containing 15 U/ml papain (Worthington Biochemical) and 0.5 mg/ml collagenase (Sigma Aldrich) and then were rinsed three times with HBSS and placed in culture Neurobasal A (Invitrogen) medium containing 2% heat-inactivated horse serum (Invitrogen), 0.2 mM L-glutamax-1 (Invitrogen), and 2% B-27 (Invitrogen). Ganglia were gently triturated with a pipette and the cell suspension was filtered with a 40 μm cell strainer. The resulting DRG neurons were plated onto poly-D-lysine- and laminin-coated coverslips or plates. Cultures were maintained for 16–72 h at 37°C in a humidified air with 5% CO_2.

Western blot analysis. Mouse DRGs were collected and homogenized using a Dounce homogenizer in an ice-cold radioimmunoprecipitation assay (RIPA) buffer containing 50 mM Tris HCl, 150 mM NaCl, 0.2 mM EDTA, 1% Triton X-100, 2% sodium dodecyl sulfate, 1% deoxycholate, 0.1 mM phenylmethanesulfonyl fluoride, and protease inhibitor cocktails (Thermo Fisher Scientific). The lysed tissues were sonicated at a constant intensity of 2.5 for 10 s and centrifuged at 12,000× *g* (4°C) for 5 min. Total protein concentrations were determined using a Pierce bicinchoninic acid protein assay kit (Thermo Fisher Scientific) following the manufacturer's instructions. Protein samples were heated at 95°C for 10 min, electrophoresed in 10% SDS polyacrylamide gel, and transferred onto nitrocellulose membranes (Bio-Rad). Blots were blocked with Odyssey blocking buffer (TBS) for 1 h at room temperature and probed with rabbit anti-Orai1 (1:1,000, AB_10692885, ProSci) and anti-β-actin (1:20,000, AB_2536382, Thermo Fisher Scientific) primary antibodies at 4°C overnight. The blots were washed and incubated for 1 h at room temperature with IRDye donkey anti-rabbit (AB_621848) or donkey anti-mouse (AB_10953628) secondary antibodies (1:10,000, LI-COR). The bands were quantified using Odyssey Image Studio software (LI-COR).

Immunofluorescence staining. Mice were deeply anesthetized with ketamine and perfused transcardially with saline, followed by 4% paraformaldehyde in 0.1 M phosphate-buffered saline, pH 7.4 (PBS). The L3 and L4 DRGs were extracted, post-fixed in 4% paraformaldehyde PBS at 4°C overnight, and then moved to 30% sucrose PBS at 4°C until immersion. The DRGs were frozen in Tissue-Tek O.C.T. compound (Sakura Finetek, VWR) on dry ice and cut into 14-μm-thick sections. DRG sections were blocked with PBS containing 5% normal goat serum (NGS) and 0.3% Triton-X 100 (blocking solution) for 1 h and were then incubated with Orai1 antibody (1:500, rabbit, AB_10692885, Prosci) in blocking solution at 4°C overnight. For double labeling, Orai1 was co-incubated with fluorescein isothiocyanate-conjugated isolectin B4 (IB4-FITC) (3 μg/ml, Sigma Aldrich), or antibodies against CGPR (1:200, goat, AB_725807, Abcam), NF200 (1:1,000, mouse, AB_477262, Sigma Aldrich), NeuN (1:100, AB_2298772, EMD Millipore), Iba-1 (1:100, AB_2820253, Sigma), or glutamine synthetase (GS, 1:200, MAB302, AB_2110656, EMD Millipore). After three washes in PBS, the sections were incubated with respective secondary antibodies (Alexa Fluor 488 or 546, Thermo Fisher) at room temperature for 1 h in the blocking solution. DRG sections were mounted onto glass slides after washing, and coverslips were applied using mounting media (SouthernBiotech) after air-drying. Images were captured using the Olympus FLUOVIEW FV1000 confocal microscope equipped with a 30× oil immersion objective.

Calcium imaging. The change of intracellular calcium (Ca^{2+}) concentration was measured as previously described (Xia et al., 2014; Wei et al., 2017). Briefly, DRG neurons seeded on coverslips were loaded with 4 μM fura-2 AM (Life Technologies) for 30 min at room temperature in HBSS, washed and further incubated in a bath solution containing (in mM) 140 choline-Cl, 10 KCl, 2 $CaCl_2$, 1 $MgCl_2$, 10 HEPES, and 10 glucose, pH 7.4, for additional 20 min. Coverslips were mounted in a small laminar-flow perfusion chamber (Model RC-25, Warner Instruments) and continuously perfused at 6–7 ml/min with the same bath solution. Images were acquired at 3 s intervals at room temperature (20–22°C) using the software MetaFluor 7.7.9 (Molecular Devices). The fluorescence ratio was determined as the fluorescence intensities excited at 340 and 380 nm with background subtraction. Only one recording was made from each coverslip. The free Ca^{2+} concentration was calculated by the formula $[Ca^{2+}] = K_d * \beta * (R - R_{min}) / (R_{max} - R)$, where $\beta = (I_{380max}) / (I_{380min})$. R_{min}, R_{max}, and β were determined by in situ calibration, as described previously (Fuchs et al., 2005), and 224 was used as the dissociation constant K_d (Grynkiewicz et al., 1985).

Electrophysiological recording. Whole-cell patch-clamp recordings were performed with an EPC 10 amplifier and PatchMaster software (HEKA Elektronik) at room temperature as described previously (Hu and Gereau, 2003). Electrode resistances were 3–5 MΩ, and most neurons had series resistance from 4 to 15 MΩ. Neurons with a resting membrane potential more hyperpolarized than −45 mV were used. For recording SOC currents in cultured DRG neurons, the electrode solution contained (in mM) 125 CsMeSO4, 8 $MgCl_2$, 10 BAPTA, 10 HEPES, 3 Na_2ATP, 0.3 Na_2GTP, and 0.002 TG, pH 7.4; the bath solution was Tyrode's solution containing (in mM) 140 NaCl, 5 KCl, 2 $CaCl_2$, 1 $MgCl_2$, 10 HEPES, and 5.6 glucose (Wei et al., 2017). A gap-free protocol was used, in which the membrane voltage was held at −70 mV without depolarization or hyperpolarization voltage pulses applied. A divalent-free (DVF) bath solution was also used for recording SOC currents, which was prepared by removing $CaCl_2$ and $MgCl_2$ from the Tyrode's solution and adding 0.1 mM EGTA (Gemes et al., 2011). For current-clamp recordings, the electrode solution contained (in mM) 140 $KMeSO_3$, 2 $MgCl_2$, 2 BAPTA, 10 HEPES, 3 Na_2ATP, 0.3 Na_2GTP, pH 7.4. The bath solution was also Tyrode's solution. Action potentials were generated by current injection from a holding potential of −65 mV. The holding potential was maintained by current injection throughout the entire recording process. The rheobase (the minimal current to evoke an action potential) was first determined for every neuron by depolarization pulses (1 s duration) ranging from 20 to 200 pA in 10 or 20 pA increments (Hu et al., 2006). Modulation of action potentials was measured every 10 s using a constant depolarization pulse (1 s, 1.2–1.5 times rheobase) throughout the recording. The amplitude that evoked two to six action potentials during the predrug period was selected and remained constant throughout the recording. The spike frequency was measured by counting the number of spikes within a 1 s depolarizing pulse. Only one DRG neuron was recorded in each coverslip.

Real-time PCR analysis of mRNA expression. Real-time PCR was conducted as described previously (Wei et al., 2017). Total RNA was extracted from DRGs using TRIzol Reagent (Molecular Research Center). The RNA concentration was detected by optical density at 260 nm. Total RNA was reverse transcribed into cDNA for each sample using a Fermentas cDNA synthesis kit (Thermo Scientific) following the manufacturer's instructions. Specific primers for mouse Orai1 (Mm00774349_m1) and GAPDH were purchased from Applied Biosystems. Real-time quantitative PCR (RT-qPCR) was performed in a 7900HT Fast Real-Time PCR System (Applied Biosystems) under the following conditions: 5 min of initial denaturation at 96°C, then 35 cycles of 96°C for 30 s, 55°C for 30 s, and 72°C for 1.5 min. The threshold cycle for each gene was determined and analyzed using the relative quantitation software (Applied Biosystems). The relative expression of the target genes was calculated using the 2(−Delta Delta CT, $2^{-\Delta\Delta CT}$) method. The mRNA level of *Orai1* was normalized to the housekeeping gene *Gapdh*.

Carrageenan-induced pain. The carrageenan pain model was generated by intraplantar injection of 2% carrageenan (15 μl) into the right hindpaw of the animal. Mechanical sensitivity was measured in both carrageenan-injected mice and PBS-injected mice before and 24 h after injection using von Frey filaments (North Coast Medical). A series of von Frey filaments were applied to both the right (ipsilateral) and left (contralateral) hindpaws of the mice. The 50% paw withdrawal threshold was determined using Dixon's up-down method (Dixon, 1980). Thermal sensitivity was detected using Hargreaves' method as previously described (Gao et al., 2015). It was also measured before and 24 h after injection in both right and left hindpaws. Paw withdrawal latency was set to ∼10 s with a maximum of 20 s as a cutoff to prevent potential injury. The latencies were averaged over three trials, separated by 30 min intervals.

CFA-induced pain. The CFA pain model was induced by intraplantar injection of 50% CFA (15 µl) into the right hindpaw. Mechanical and thermal sensitivity was measured before CFA injection and 3 h, 24 h, 72 h, and 7 d after CFA injection using von Frey filaments and Hargreaves' method mentioned above. Paw thickness was measured at the midplantar level before CFA injection and 3 h, 24 h, 72 h, and 7 d after CFA injection (after the Hargreaves' test) by an electronic caliper (World Precision Instruments) as previously described (Boettger et al., 2007; Dou et al., 2018). Paw edema was determined by subtracting the paw thickness measured before CFA injection from that measured after injection. Weight distribution on each hindlimb was measured before CFA injection and 5 and 24 h after CFA injection (after the von Frey filaments test) using an incapacitance analgesia meter (IITC Life Science). Mice were placed into an angled plexiglass chamber of the incapacitance meter with their hindpaws on separate sensors. Each data point is the average of three readings. Data were expressed as the difference (g) of weight distribution between ipsilateral and contralateral hindlimbs.

PGE2-induced pain hypersensitivity. PGE2 (0.3 nmol) was injected into the plantar surface of the right hindpaw of the testing mice to induce pain hypersensitivity. Mechanical and thermal sensitivity was measured before injection of PGE2 and 1 h after injection using von Frey filaments and Hargreaves' method mentioned above.

Measurement of TNF-α, IL-1β, and PGE2 in the injected paw. Mice were anesthetized 7 d after CFA or PBS injection (after the behavior tests). The entire injected paw was collected, and both dorsal and plantar surfaces were incised multiple times. The paw was placed in a 12-well plate containing 20 µg/ml indomethacin (PBS) and gently shaken at 100 rpm for 1 h. After that, the tissue samples were centrifuged at 10,000 rpm for 10 min, and the supernatant was then collected for the assay. TNF-α, IL-1β, and PGE2 concentrations in the supernatant were measured by ELISA according to the manufacturer's instructions (R&D Systems).

Drug application. Thapsigargin (TG), carrageenan, CFA, and PGE2 were purchased from Sigma Aldrich. ML-9, U73122, GF109203X, and KT5720 were purchased from Tocris. SC19220, 17-pt-PGE2, and L161982 were purchased from Cayman Chemical. FR900395 was kindly provided by Professor Kendall Blumer from Washington University School of Medicine in St. Louis, MO. They were dissolved in Milli-Q water or dimethyl sulfoxide (DMSO) as stock solutions and further diluted to final concentrations in 0.1% DMSO.

Statistical analysis. Original traces represent raw data recorded with the specific software. Offline data analysis was processed using PatchMaster (HEKA) and Origin 8.1 software (OriginLab). Summary data are expressed as mean ± SEM. Treatment effects were statistically analyzed by Origin 8.1 software with a one-way analysis of variance (ANOVA). When ANOVA showed a significant effect, pairwise comparisons between means were performed by post hoc Tukey's test except where otherwise noted. Paired or two-sample Student's *t* tests were used when comparisons were restricted to two means.

Results

Orai1 deficiency impairs SOCE and SOC currents in DRG neurons

We have demonstrated that Orai1 is an important component of SOCs in DRG neurons using the small inhibitory RNA (siRNNA) knockdown approach (Wei et al., 2017). To further characterize the distribution and function of Orai1 in DRG neurons, we took advantage of our Orai1 mutant mouse model, which has been described previously (Dou et al., 2018). Western blot analysis showed that Orai1 was not detectable in the DRGs from Orai1 KO mice (Extended Data Fig. 1-1*A*). Immunostaining of DRG sections also showed that Orai1 was absent in the DRG from Orai1 KO mice (Extended Data Fig. 1-1*B*). Using the same Orai1 antibody, we observed that Orai1 was widely expressed, but relatively highly expressed in IB4- and CGRP-positive neurons than NF200-positive neurons (Fig. 1*A–C*). We also examined Orai1 expression in satellite glial cells (SGCs) and local macrophages. Orai1 was neither co-stained with GS, a known marker of SGCs (Miller et al., 2002; Laursen et al., 2014), nor co-expressed with Iba-1, a marker of local macrophages (Extended Data Fig. 1-2). Consistent with our previous Orai1 knockdown results obtained by using siRNA transfection (Wei et al., 2017), TG (an ER Ca^{2+}-ATPase inhibitor)-induced SOCE was largely attenuated in DRG neurons from Orai1 global KO mice when compared with neurons from their littermate WT mice by calcium imaging (Fig. 1*D*). Further, whole-cell patch-clamp recordings were also performed as described recently (Wei et al., 2017). Briefly, the DRG neurons were held at −70 mV, and a gap-free recording protocol was used. SOC currents were induced by intracellular application of BAPTA and TG. DRG neurons were clamped for at least 5 min under the 2 mM Ca^{2+} Tyrode's solution to activate SOCs. Since SOC currents were small in the presence of Ca^{2+}, we used a DVF solution to induce robust monovalent I_{CRAC} (DeHaven et al., 2007; Gemes et al., 2011). Once the SOC currents reached maximal levels, 2 mM Ca^{2+} Tyrode's solution was used to wash off DVF solution. DRG neurons from Orai1 KO mice showed a significant decrease in BAPTA/TG-induced SOC currents compared with those from WT mice (Fig. 1*E*). These results suggest that Orai1 is a key component mediating SOCE and SOC currents in DRG neurons.

Orai1 deficiency attenuates CFA-induced pain hypersensitivity

We have reported that Orai1 deficiency significantly attenuates carrageenan-induced acute pain hypersensitivity (Dou et al., 2018). To determine whether Orai1 plays a key role in CFA-induced pain hypersensitivity, CFA was injected into the plantar of right hindpaws of WT and their littermate Orai1 KO mice. WT mice developed significant mechanical hypersensitivity in the ipsilateral (Ipsi) but not contralateral (Contra) paws 3, 24, and 72 h and 7 d after CFA injection, which was robustly reduced in their Orai1 KO littermates (Fig. 2*A*). Thermal hypersensitivity was also developed in the ipsilateral paw of WT mice after CFA injection, which was attenuated in Orai1 KO mice (Fig. 2*B*). To further confirm that Orai1 is involved in CFA-induced pain, we examined weight-bearing as an alternative nonreflex readout. CFA injection resulted in impaired weight distribution between ipsilateral and contralateral paws from WT mice, which was largely reduced at earlier time points and absent after 3 d from Orai1 KO mice (Fig. 2*C*). This observation led us to test whether Orai1 is involved in CFA-induced peripheral inflammation; thus, we measured paw thickness and inflammatory mediator concentration in the injected paw. Interestingly, CFA-induced changes in paw thickness and inflammatory mediator production were unaltered in Orai1 KO compared with WT mice (Fig. 2*D–G*). These results indicated that Orai1 plays an important role in CFA-induced pain but not inflammation.

Deletion of Orai1 in advillin-expressing cells diminishes CFA-induced pain hypersensitivity

To determine the functional role of Orai1 in CFA-induced peripheral sensitization, we recently generated advillin expressing cell-specific Orai1 KO mice [$Advillin^{Cre/+}$;$Orai1^{flox/flox}$ (Adv-Orai1 KO)] by crossing female $Orai1^{flox/flox}$ mice with male $Advillin^{Cre/+}$ knock-in mice (Fig. 3*A*), in which Cre recombinase is primarily expressed in the primary sensory neurons

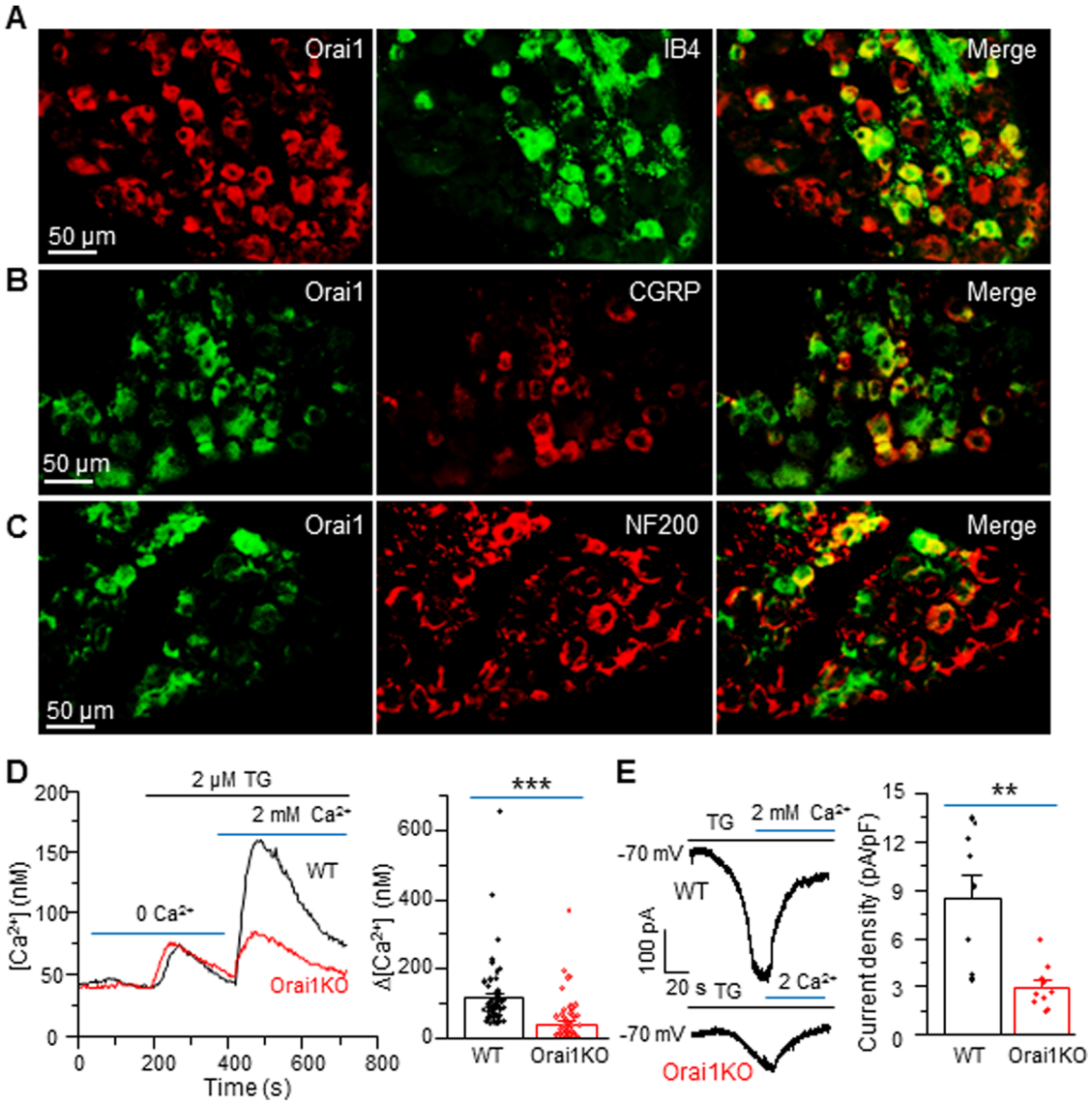

Figure 1. Orai1 deficiency abolishes SOCE and SOC currents in DRG neurons. ***A–C***, Confocal images of co-immunostaining of Orai1 with IB4 (***A***), CGRP (***B***), or NF200 (***C***) in DRG sections from WT mice. ***D***, TG-induced Ca^{2+} entry in DRG neurons from WT and Orai1 KO mice, WT, $n = 59$ neurons; KO, $n = 75$ neurons from 2 cultures. ***E***, TG-induced SOC currents in DRG neurons from WT and Orai1 KO mice, WT, $n = 9$ neurons, from 3 cultures; Orai1KO, $n = 10$ neurons, from 2 cultures. Values represent mean ± SEM; $^{**}p < 0.01$, $^{***}p < 0.001$, compared with WT by Student's *t* test. See Extended Data Figures 1-1, 1-2.

(Zurborg et al., 2011). Adv-Orai1 KO mice were indistinguishable in size and body weight from WT littermates (data not shown). Western blot analysis showed that Orai1 was markedly reduced in the DRG, but not the spinal cord from Adv-Orai1 KO mice (Fig. 3*B*). The immunostaining result further confirmed the large reduction (87%) of Orai1 positive neurons in the DRG (Fig. 3*C*). Basal mechanical and thermal sensitivities were not altered in Adv-Orai1 KO mice (Fig. 3*D*,*E*), whereas CFA-induced mechanical and thermal hypersensitivities were significantly decreased in Adv-Orai1 KO mice compared with their WT littermates (Fig. 3*D*,*E*). These data further demonstrate that Orai1 plays an important role in peripheral sensitization associated with inflammatory pain.

Orai1-mediated SOCE is increased in DRG neurons from carrageenan-injected mice

To determine whether Orai1 expression in DRGs was altered under inflammatory conditions, 2% carrageenan (15 μl) was injected into the plantar of the right hindpaw of WT mice. Mechanical and thermal sensitivities were evaluated before and 24 h after carrageenan injection. The mice developed robust hypersensitivity to mechanical and thermal stimuli in the ipsilateral paws 24 h after injection of carrageenan (Extended Data Fig. 4-1*A*,*B*). Both ipsilateral and contralateral L3/4 DRGs were collected after behavior tests, and RT-qPCR was performed. Our results showed that Orai1 mRNA level was not altered in the ipsilateral L3/4 DRGs (Extended Data Fig. 4-1*C*).

To assess whether SOC function was altered in carrageenan-injected mice, ipsilateral L3 and L4 DRGs were collected 24 h after carrageenan or PBS injection, and then DRG neurons were harvested and cultured. Calcium imaging recordings were performed on these neurons 2–6 h after harvest. TG-induced SOCE was significantly increased in DRG neurons from carrageenan-injected mice (Fig. 4*A*,*B*). Further, whole-cell patch-clamp recordings were performed on these neurons. Neurons were held at −70 mV, and the same protocol was conducted as

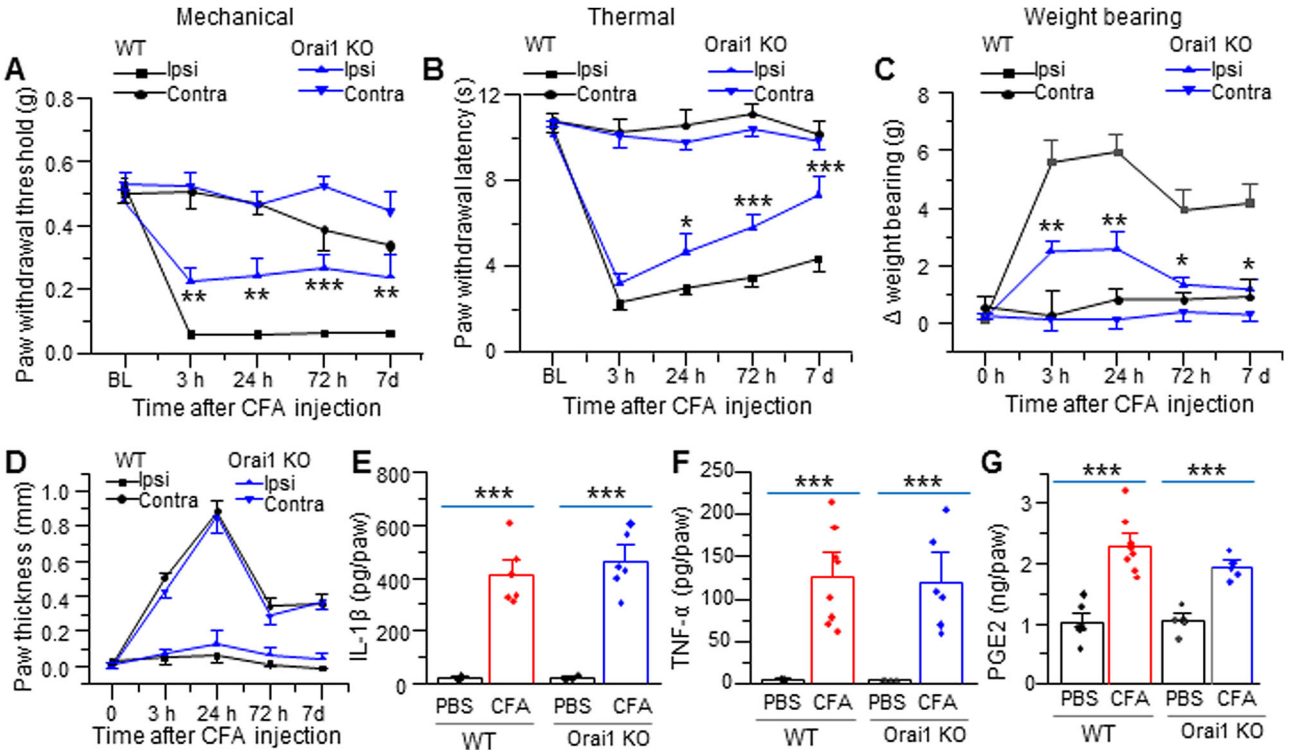

Figure 2. Orai1 deficiency attenuates CFA-induced pain hypersensitivity. ***A***, ***B***, Effects of deficiency of Orai1 on CFA-induced mechanical allodynia (***A***) and thermal hyperalgesia (***B***). For mechanical allodynia, WT, $n = 8$ mice; KO, $n = 6$ mice; for thermal hyperalgesia, WT, $n = 10$ mice; KO, $n = 9$ mice. ***C***, ***D***, Effects of deficiency of Orai1 on CFA-induced weight-bearing impairment (***C***) and paw edema (***D***), WT, $n = 8$ mice; KO, $n = 6$ mice. ***E–G***, Effects of deficiency of Orai1 on CFA-induced IL-1β (***E***), TNF-α (***F***), and PGE2 (***G***) production, WT, $n = 8$ mice; KO, $n = 7$ mice. Values are means ± SEM; $*p < 0.05$, $**p < 0.01$, $***p < 0.001$ compared with WT or PBS by two-way repeated measures ANOVA (***A–C***) or one-way ANOVA (***E–G***) with Tukey's test.

described above. ML-9, an Orai channel antagonist, was used after SOC current induction to evaluate SOC currents (Wei et al., 2017). BAPTA/TG-induced SOC currents were markedly increased in DRG neurons from carrageenan-injected mice compared with PBS group (Fig. 4*C*,*D*). These results further indicate that SOCs are involved in inflammation-induced peripheral sensitization.

To determine whether the SOC functional changes are mediated by Orai1, 2% carrageenan was injected into the plantar of the right hindpaw of both Orai1 KO and WT mice. Consistent with our previous report (Dou et al., 2018), deletion of Orai1 attenuated carrageenan-induced pain hypersensitivity (data not shown). Ipsilateral L3/4 DRGs were collected and cultured 24 h after carrageenan or PBS injection, and neurons were subjected to calcium imaging or whole-cell patch-clamp recordings 2–6 h after harvest. Interestingly, carrageenan-induced increase in SOCE and SOC currents were abolished in L3/4 DRG neurons from Orai1 KO mice (Fig. 4*E–H*). These results indicate that acute inflammation-induced SOCE increase is mediated by Orai1.

Orai1-mediated SOCE is increased in DRG neurons at an earlier timepoint after CFA injection

To determine whether Orai1 expression is altered after CFA injection, Western blotting was performed with the L3/4 DRGs from the WT mice collected 24 h or 7 d after CFA injection. Similarly, Orai1 protein level in ipsilateral L3/4 DRGs from CFA-injected mice (both 24 h and 7 d after injection) did not differ from those obtained from PBS-injected mice (Fig. 5*A*,*B*), suggesting that CFA-induced inflammatory pain does not affect the expression of Orai1 in DRGs.

To determine whether SOC function is altered in DRGs from CFA-induced mice, ipsilateral L3/4 DRGs from WT mice were collected 24 h after CFA injection, and the cultured neurons were subjected to calcium imaging 2–6 h after harvest. TG-induced SOCE was significantly increased in DRG neurons from CFA-injected WT mice (Fig. 5*C*,*D*). Interestingly, this increase in SOCE was not observed in L3/4 DRG neurons from Orai1 KO mice (Fig. 5*E*,*F*). We also collected ipsilateral L3/4 DRGs from WT mice 7 d after CFA injection and conducted calcium imaging. However, there was no difference in TG-induced SOCE between the CFA-injected group and PBS-injected group 7 d after injection (Fig. 5*G*,*H*). These results suggest that Orai1 may play a role in inflammatory pain initiation.

PGE2 potentiates Orai1-mediated SOCE in DRG neurons

Since Orai1 functional change was not associated with increase in its expression, we wondered whether the change was due to the modulation of Orai1 function. It was previously reported that PGE2 is produced in inflamed tissues and can lead to sensitization of DRG neurons and subsequent hyperalgesia (Moriyama et al., 2005; Sachs et al., 2009). Therefore, we sought to determine whether PGE2 can modulate the function of SOCs in DRG neurons. To test the effect of PGE2 on SOCE in DRG neurons, the DRG neurons were pretreated with vehicle (0.1% DMSO) or PGE2 for 5 min, TG-induced Ca^{2+} entry was recorded in the presence of vehicle or PGE2. We compared the effect of PGE2 at three different concentrations, which were chosen based on previous studies (Vasko et al., 2014; Jang et al., 2017; Ma et al., 2017), TG-induced SOCE was not affected by the lower concentration (0.2 μM), while pretreatment with either 1 or 5 μM of PGE2 significantly increased SOCE in DRG neurons (Fig. 6*A*,*B*). There was no difference between 1 and 5 μM PGE2 treatment. This result demonstrates that PGE2 potentiates TG-induced SOCE in DRG neurons.

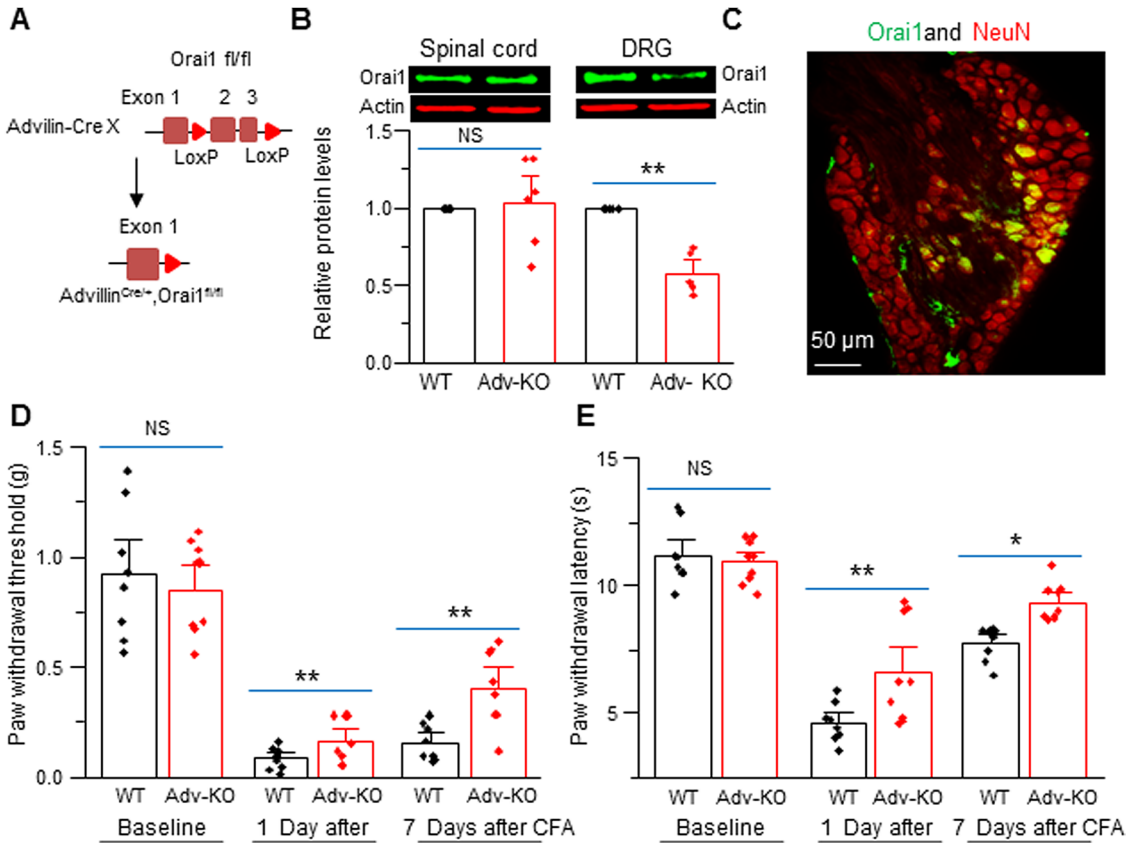

Figure 3. Deletion of Orai1 in advillin-expressing neurons attenuates CFA-induced pain hypersensitivity. ***A***, Schematic of the targeting strategy for conditional deletion of Orai1. ***B***, Western blot analysis of Orai1 protein extracted from DRG and spinal cord tissues of WT and Advillin-Orai1 knockout (Adv-KO) adult mice, WT, $n = 5$ mice; KO, $n = 6$ mice. ***C***, A confocal image of co-immunostaining of Orai1 (green) and NeuN (red) in DRGs from Adv-Orai1 KO adult mice. ***D***, ***E***, Effects of deficiency of Orai1 in advillin-expressing neurons on CFA-induced mechanical allodynia (***D***) and thermal hyperalgesia (***E***) at two timepoints (WT, $n = 8$ mice; KO, $n = 9$ mice). Values represent mean ± SEM; $*p < 0.05$, $**p < 0.01$ compared with WT by one-way ANOVA.

To determine whether PGE2-induced increase in SOCE is mediated by Orai1, we cultured DRG neurons from adult Orai1 KO mice. Calcium imaging was performed following incubation of the neurons with vehicle or 1 μM PGE2 before TG-induced Ca^{2+} entry was triggered. We found that TG-induced SOCE was indistinguishable between vehicle-pretreated and PGE2-pretreated neurons (Fig. 6*C*,*D*). To further confirm that PGE2 enhanced SOC function, patch-clamp recordings were conducted in DRG neurons from WT and Orai1 KO mice. Consistently, TG-induced SOC currents were increased after PGE2 treatment in WT neurons. This increase was not observed in Orai1 KO neurons (Fig. 6*E*,*F*), suggesting that PGE2 potentiates Orai1-mediated SOCE.

Orai1 contributes to PGE2-induced increase in neuronal excitability and pain hypersensitivity

We have shown that SOC activation increases neuronal excitability (Wei et al., 2017). To determine whether Orai1 is involved in PGE2-induced increase in neuronal excitability, we performed current-clamp recordings in cultured DRG neurons from Orai1 KO and WT mice using an internal recording solution containing 2 mM BAPTA. The resting membrane potential in WT neurons was −51.5 ± 1.0 mV, while it was −50.8 ± 1.2 mV in Orai1 KO neurons ($n = 28$ each; $p = 0.655$). The basal rheobase was indistinguishable between WT and Orai1 KO neurons (Fig. 7*A*). Bath application of PGE2 significantly increased the rheobase in WT, but not in Orai1 KO neurons (Fig. 7*B*). The firing rate was markedly increased in 13 out of 20 neurons recorded in WT neurons and 7 out of 19 in Orai1 KO neurons (Fig. 7*C*–*E*). These results indicate that Orai1 is involved in PGE2-induced increase in neuronal excitability.

To determine whether Orai1 was involved in PGE2-induced pain hypersensitivity, an in vivo study was performed. Basal mechanical and thermal sensitivities were measured before and after 0.3 nmol PGE2 intraplantar injection. WT mice developed robust mechanical and thermal hypersensitivity in their ipsilateral paws within 1 h after PGE2 injection, while both mechanical allodynia and thermal hyperalgesia were significantly diminished in Orai1 KO mice (Fig. 7*F*,*G*), suggesting that Orai1 plays a crucial role in PGE2-induced pain hypersensitivity.

PGE2-induced increase in SOCE is mediated by EP1 in DRG neurons

PGE2 exerts modulatory effects by acting through four G-protein-coupled receptors (EP1-4). Previous studies have shown that EP1 and EP4 are more prominent than EP2 and EP3 in mediating the effect of PGE2 in primary sensory neurons and contributing to inflammatory and neuropathic pain (Ma et al., 2010; Cruz Duarte et al., 2012). To determine whether the effect of PGE2 is mediated by EP1 or EP4, DRG neurons were incubated in extracellular solution containing 20 μM SC19220 (EP1 antagonist) or 1 μM L161982 (EP4 antagonist) for 10 min before calcium imaging, and the specific antagonists were present during the entire recordings (Yang et al., 2015a,b, 2017; Varga et al., 2016; Ma et al., 2017). We found that blockade of EP1 but not EP4 receptor completely attenuated PGE2-induced increase in SOCE in DRG

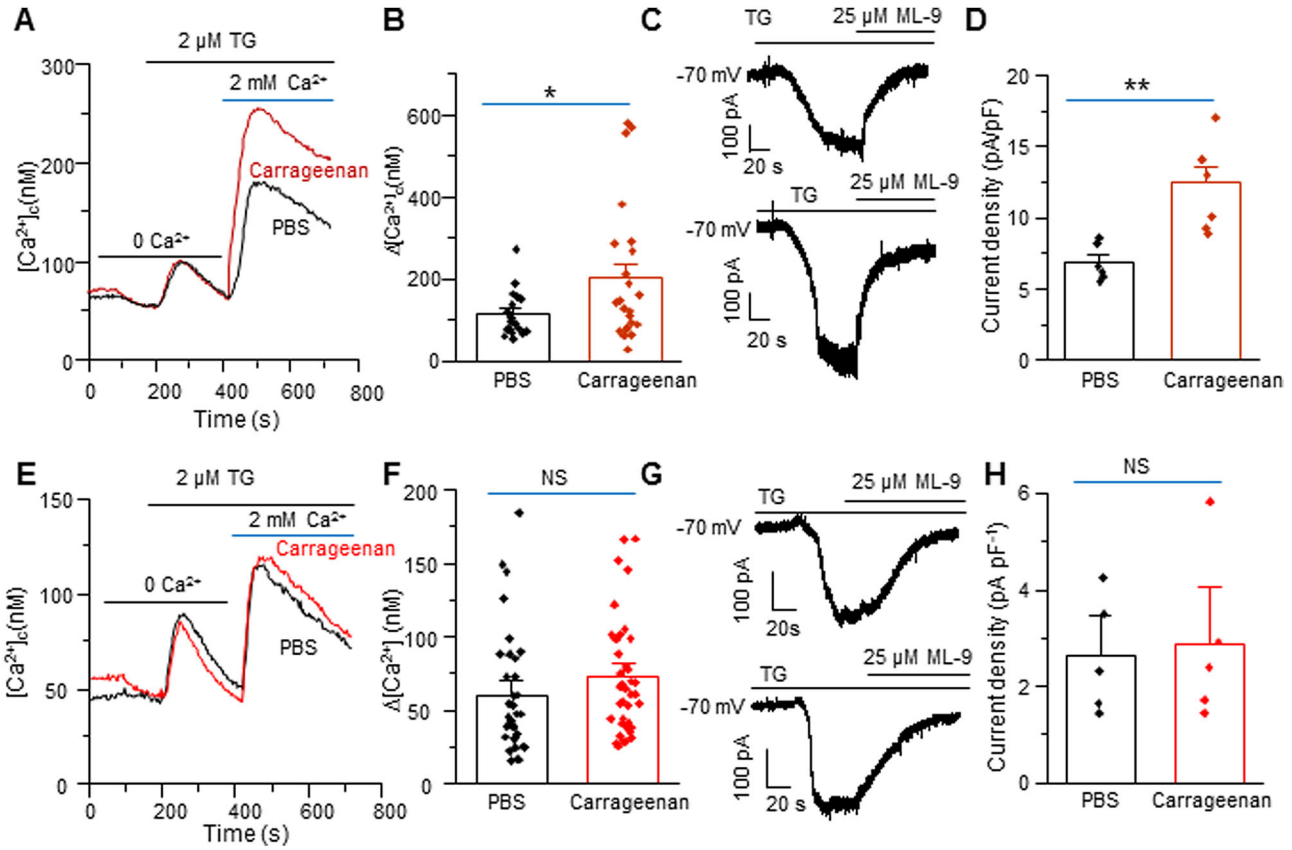

Figure 4. Orai1-mediated SOCE and SOC currents are increased in DRG neurons from carrageenan-injected mice. ***A***, Representative recordings of TG-induced SOCE in ipsilateral L3/L4 WT DRG neurons from PBS or carrageenan-injected mice. ***B***, Effect of carrageenan injection on SOCE in DRG neurons from WT mice (PBS: $n = 18$ neurons from 2 cultures; carrageenan: $n = 24$ neurons from 2 cultures). ***C***, Representative recordings of TG-induced SOC currents in ipsilateral L3/L4 DRG neurons from PBS or carrageenan-injected mice. ***D***, Effect of carrageenan injection on SOC currents in DRG neurons from WT mice (PBS, $n = 6$ neurons from 2 cultures; carrageenan, $n = 7$ neurons from 2 cultures). ***E***, Representative recordings of TG-induced SOCE in ipsilateral L3/L4 DRG neurons from Orai1 KO mice injected with PBS or carrageenan. ***F***, Effect of carrageenan injection on SOCE in DRG neurons from Orai1 KO mice, $n = 35$ neurons from 4 cultures; carrageenan, $n = 43$ neurons from 4 cultures. ***G***, Representative recordings of SOC currents in ipsilateral L3/L4 DRG neurons from Orai1 KO mice injected with PBS or carrageenan. ***H***, Effect of carrageenan injection on SOC currents in DRG neurons from Orai1 KO mice, $n = 5$ neurons, each group from 3 mice (2 cultures). Values represent mean ± SEM; $^*p < 0.05$, $^{**}p < 0.01$ compared with control by Student's *t* test. See Extended Data Figure 4-1.

neurons (Fig. 8*A*,*B*). We also measured SOC currents in the presence of SC19220. PGE2-induced increase in SOC currents was not observed in SC19220-treated compared with vehicle-treated neurons (Fig. 8*C*,*D*). To confirm that activation of EP1 can increase SOCE, we used 17-pt-PGE2, an agonist of EP1 (Leclerc et al., 2015). Neurons were pretreated with vehicle or 17-pt-PGE2 for 5 min. TG-induced SOCE was increased in the 17-pt-PGE2-treated compared with the vehicle-treated group (Fig. 8*E*,*F*). These findings suggest that PGE2-induced modulation of Orai1 is mediated by EP1.

Since EP1 is a Gq-coupled receptor, we wondered whether activation of EP1 can induce Ca^{2+} release from the ER and neurons were perfused with Ca^{2+}-free NMDG-based Tyrode's solution. 17-pt-PGE2-induced intracellular Ca^{2+} release was only observed in 7 neurons (out of 388 neurons recorded, 1.8%). Surprisingly, subsequent addition of 2 mM calcium resulted in robust Ca^{2+} influx in 130 neurons (33.5%). In contrast, neurons treated with vehicle (0.1% DMSO) showed no Ca^{2+} release from the ER under the Ca^{2+}-free condition, and 2 mM Ca^{2+} addition led to small Ca^{2+} influx (Extended Data Fig. 8-1*A*,*B*). To determine whether this effect is neuronal subtype-specific, neurons were incubated with fluorescein isothiocyanate-conjugated isolectin B4 (IB4-FITC, 10 μg/ml) for 10 min after recording. The 17-pt-PGE2's effect occurred in both IB4+ and IB4− neurons (Extended Data Fig. 8-1*C*,*D*). The 17-pt-PGE2-induced increase in Ca^{2+} influx was significantly attenuated by YM-58483 (an Orai1 blocker) and ML-9 (a STIM1 inhibitor), respectively (Extended Data Fig. 8-2*A*,*B*). To further confirm that 17-pt-PGE2-induced increase in Ca^{2+} influx was mediated by Orai1, we repeated this experiment in WT and Orai1 KO neurons. Consistently, the 17-pt-PGE2-induced increase in Ca^{2+} influx was largely attenuated in Orai1 KO neurons (Fig. 8*G*,*H*), although 11 out of 185 neurons (6%) still showed some Ca^{2+} influx. These findings further indicate that EP1 activation enhances Orai1-ediated Ca^{2+} influx.

PGE2-induced increase in SOCE is mediated by the Gq-PKC and ERK pathway(s) in DRG neurons

Since EP1 is coupled to Gq/11 class G-proteins, we determine whether the effect of PGE2 is mediated by Gq/11 signaling and DRG neurons were pretreated with 100 nM FR900359, a Gq/11-specific inhibitor (Kamato et al., 2017; Crusemann et al., 2018), for 10 min before calcium imaging. As expected, inhibition of Gq/11 protein abolished PGE2-induced SOCE increase in DRG neurons (Fig. 9*A*,*B*), while incubation with FR900359 itself had no effect on SOCE (data not shown).

It is well known that EP1 is linked to a stimulatory pathway that activates PKC. To determine whether PKC is involved in PGE2-mediated potentiation of SOCE, we pretreated DRG neurons with 0.5 μM GF109203X (PKC inhibitor) prior to

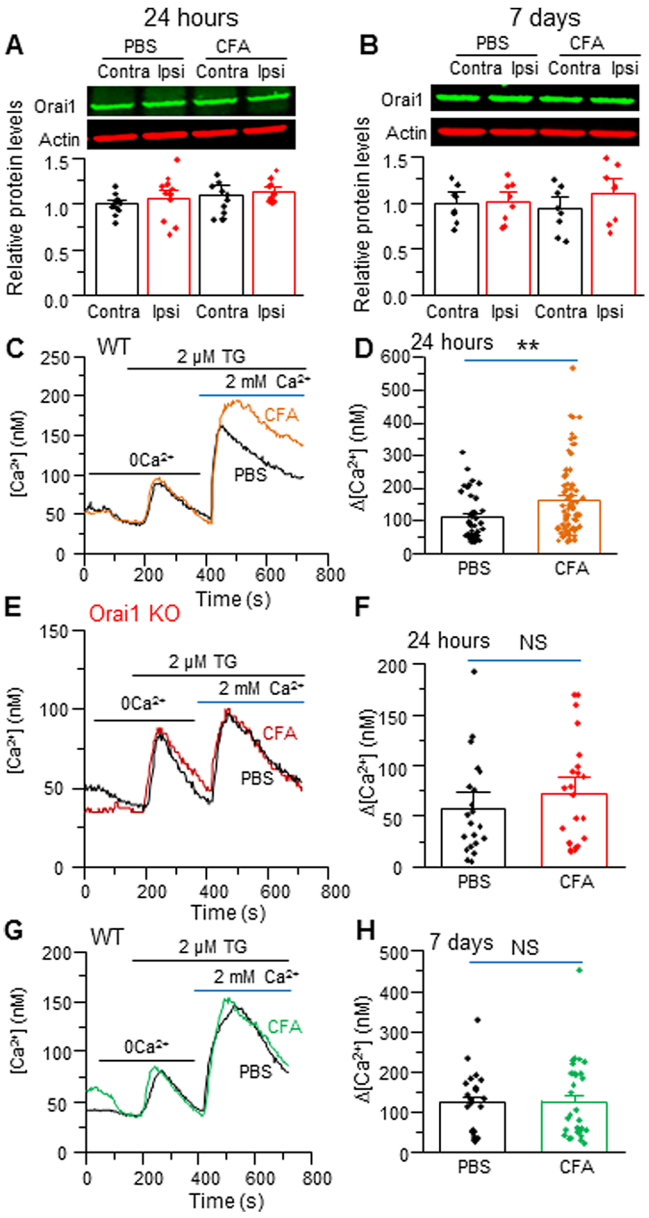

Figure 5. Orai1-mediated SOCE is increased in DRG neurons from CFA-injected mice. ***A***, ***B***, Orai1 protein levels in ipsilateral L4 and L5 DRGs from PBS- and CFA-injected mice 24 h (***A***) and 7 d (***B***) after injection (24 h, $n = 12$ mice; 7 d, $n = 8$ mice). ***C***, Representative recordings of TG-induced SOCE in ipsilateral L3/L4 WT DRG neurons from PBS- and CFA-injected WT mice 24 h after injection. ***D***, Effect of CFA injection on SOCE of ***C***, PBS, $n = 43$ neurons from 2 cultures; CFA, $n = 70$ neurons from 2 cultures. ***E***, Representative recordings of SOCE in ipsilateral L3/L4 DRG neurons from PBS- and CFA-injected Orai1 KO mice 24 h after injection. ***F***, Effect of CFA injection on SOCE of ***E***, PBS, $n = 21$ neurons from 2 cultures; CFA, $n = 23$ neurons from 2 cultures. ***G***, Representative recordings of TG-induced SOCE in ipsilateral L3/L4 DRG neurons from PBS- and CFA-injected WT mice 7 d after injection. ***H***, Effect of CFA injection on SOCE of ***H***, PBS, $n = 26$ neurons from 2 cultures; CFA, $n = 32$ neurons from 2 cultures. Values represent mean ± SEM; $^{**}p < 0.01$ compared with control by Student's *t* test.

calcium imaging for 10 min (Hu et al., 2003; Wang et al., 2012; Dou et al., 2018). Inhibition of PKC completely blocked PGE2-induced SOCE increase (Fig. 9*C*,*D*). In contrast, inhibition of PKA activity with 1 μM KT5720 had no effect on PGE2-induced increase in SOCE in DRG neurons (Fig. 9*E*,*F*). Treatment with the inhibitors alone did not affect TG-induced SOCE in DRG neurons (data not shown). It is known that ERK can be activated by PGE2 (Cruz Duarte et al., 2012; Ma et al., 2017). We further tested the effects of MEK/ERK inhibitors PD98059 and U0126 on PGE2-induced modulation of SOCE. Both PD98059 and U0126 did not alter SOCE (data not shown) but eliminated PGE2-induced enhancement of SOCE (Fig. 9*G*,*H*). These results indicate that PGE2 modulates SOC function via the EP1-Gq-PKC and ERK pathway(s), rather than the EP4-PKA pathway.

Discussion

Findings from the present study show that Orai1 is expressed in nociceptors, and Orai1 deficiency in sensory neurons diminishes CFA-induced pain hypersensitivity, demonstrating an important role of Orai1 in peripheral sensitization associated with inflammatory pain. Calcium imaging and patch-clamping results reveal that SOC function is enhanced in DRG neurons under inflammatory conditions. Our results also provide the first evidence that PGE2 potentiates Orai1-mediated SOCE and SOC currents in DRG neurons through the EP1 and its downstream signaling pathway. More importantly, Orai1 plays a crucial role in PGE2-induced mechanical and thermal hyperalgesia.

We have demonstrated that Orai1 is expressed and functional in DRG neurons by using the siRNA approach (Wei et al., 2017). Here we further examined its distribution and contribution to SOCE in DRG neurons. Orai1 is widely expressed in DRG neurons with relatively high expression in nociceptors. Our functional assays revealed that SOCE and SOC currents were largely reduced, but not eliminated, in Orai1 KO DRG neurons, demonstrating that Orai1 is the key component mediating SOCE in DRG neurons. Based on our previous report (Wei et al., 2017), the residual SOCE and currents could be mediated by Orai3, a member of the SOC family. We wondered whether nociceptor Orai1 is involved in inflammation-mediated peripheral sensitization. By taking advantage of available global Orai1 KO mice, we found that CFA-induced mechanical and thermal hypersensitivities were markedly reduced in Orai1 KO mice. However, CFA-induced inflammation was not affected, which is consistent with what we found in carrageenan-induced inflammatory pain model (Dou et al., 2018). This result further confirms that Orai1 is dispensable in peripheral inflammation. Since global targeting of Orai1 in mice could not differentiate between central and peripheral contributions, we generated advillin-expressing cell-specific Orai1 KO mice in which Orai1 expression was reduced in the DRG, but intact in the spinal cord. The Orai1 conditional KO mice also showed a significant reduction in CFA-induced pain hypersensitivity. Because a previous study reported that advillin is expressed in other cell types/tissues and a few areas in the brain (Hunter et al., 2018), the possibility that Orai1 plays a role in pain hypersensitivity in those tissues could not be ruled out.

Our calcium imaging and patch-clamping data show that TG-induced SOCE and SOC currents were significantly increased in DRG neurons from carrageenan- and CFA-injected mice 24 h after injection. We have demonstrated that the SOC function is mediated by both Orai1 and Orai3 in DRG neurons (Wei et al., 2017). Interestingly, the enhanced SOC function was eliminated in Orai1 KO DRG neurons, suggesting that Orai1 solely mediates this enhancement. Unexpectedly, Orai1 protein level in DRGs was not altered in carrageenan- or CFA-induced inflammatory pain models, indicating that Orai1 may undergo functional modification during the inflammatory process. More interestingly, there was no difference in SOCE between vehicle-treated group and the CFA-treated group 7 d

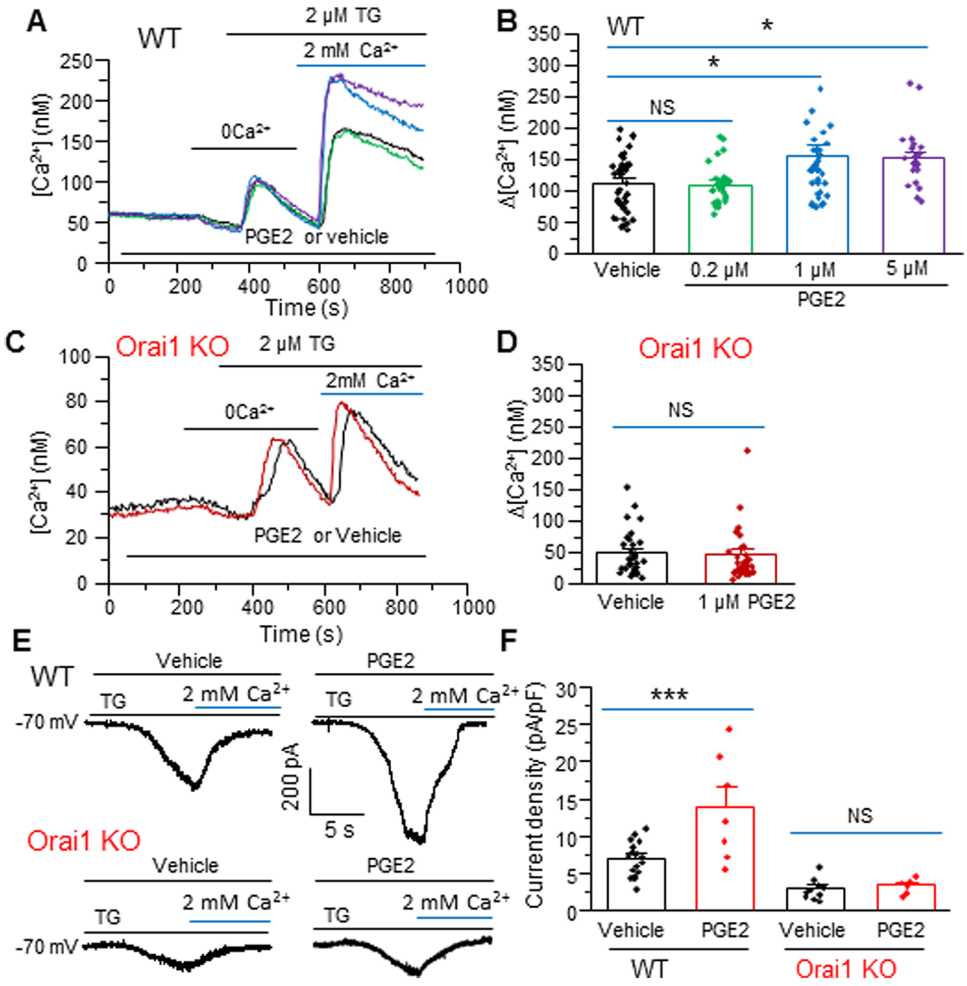

Figure 6. PGE2 application enhances Orai1-mediated Ca^{2+} entry and currents in DRG neurons. ***A***, Representative traces of SOCE in WT DRG neurons treated with different concentrations of PGE2 or vehicle (0.1% DMSO). ***B***, Effect of PGE2 on SOCE in WT DRG neurons, vehicle, $n = 43$ neurons; 0.2 μM PGE2, $n = 26$ neurons; 1 μM PGE2, $n = 34$ neurons; 5 μM PGE2, $n = 20$ neurons from 2 cultures. ***C***, Representative traces of SOCE in DRG neurons from Orai1 KO mice treated with vehicle or 1 μM PGE2. ***D***, Effect of PGE2 on SOCE in Orai1 KO neurons, PBS, $n = 32$ cells; 1 μM PGE2, $n = 41$ cells from 2 cultures. ***E***, Representative recordings of SOC currents in DRG neurons treated with vehicle or PGE2. ***F***, Effect of PGE2 on SOC currents in WT and Orai1 KO neurons, vehicle, $n = 18$ neurons (WT), $n = 10$ neurons (KO); PGE2, $n = 7$ neurons (WT), $n = 6$ neurons (KO) from 9 cultures in total. Values represent mean ± SEM; $*p < 0.05$ compared with control, $***p < 0.001$ compared with WT vehicle by one-way ANOVA with Fisher's test (***B***) and Student's *t*-test (***D***, ***F***).

after CFA injection, although reduction in pain hypersensitivity was still observed 7 d after CFA injection. These results suggest that Orai1 might be involved in pain initiation and subsequently impacts its downstream effectors in later timepoints.

PGE2 induces robust pain hypersensitivity (Yang and Gereau, 2002; Kassuya et al., 2007). Our data showed that PGE2-induced pain hypersensitivity was significantly reduced in Orai1 KO mice, indicating that Orai1 may be a downstream target of PGE2. Consistently, our in vitro study revealed that PGE2-induced increase in neuronal excitability was also markedly decreased in Orai1 KO DRG neurons compared with WT DRG neurons. This result provides a functional link between PGE2 and Orai1. It is well known that PGE2 can sensitize the peripheral terminals of nociceptors by increasing voltage-gated Ca^{2+} currents and Na^{+} currents and potentiating TRPV1 functions (Gold et al., 1996; Lopshire and Nicol, 1998; Smith et al., 2000; Rush and Waxman, 2004; Moriyama et al., 2005); we therefore tested whether PGE2 can directly modulate SOCs. Our results showed that PGE2 potentiated SOCE and SOC currents in DRG neurons, which was eliminated when Orai1 was absent in DRG neurons, suggesting that PGE2 enhances Orai1-mediated Ca^{2+} signal. Previous studies have indicated that PGE2 sensitizes nociceptors via its receptors expressed in DRG neurons (Ma, 2010; Ma et al., 2010). It has been shown that EP1 and EP4 play a major role in inflammatory pain mediation (Lin et al., 2006; Clark et al., 2008; Ma et al., 2010; Cruz Duarte et al., 2012). Evidence has suggested that both PKC and PKA signaling cascades in DRG neurons are involved in the PGE2-induced inflammatory pain and hyperalgesia (Moriyama et al., 2005; Lin et al., 2006; Sekiguchi et al., 2013). EP1 couples to Gq/11 to activate PKC signaling while EP4 activates cAMP/PKA-dependent signaling by coupling to Gs class G-protein (Alfranca et al., 2006). To understand how PGE2 potentiates SOC function, specific antagonists for EP1 and EP4 were applied to pretreat the DRG neurons before calcium imaging was conducted. Pretreatment with EP1 antagonist but not EP4 antagonist completely abolished PGE2-induced increase in SOCE in DRG neurons. The activation of EP1 by 17-pt-PGE2 also produced a similar effect, suggesting that PGE2 exerts its effect on SOCs through EP1. It has been shown that 17-pt-PGE2 also activates EP3 (Theiler et al., 2016). The increased SOCE is unlikely mediated by EP3 because activation of EP3 leads to antinociception and produces an inhibitory effect on PGE2-induced modulation of TTX-R Na^{+} currents (Bar et al., 2004; Konig et al., 2022). To

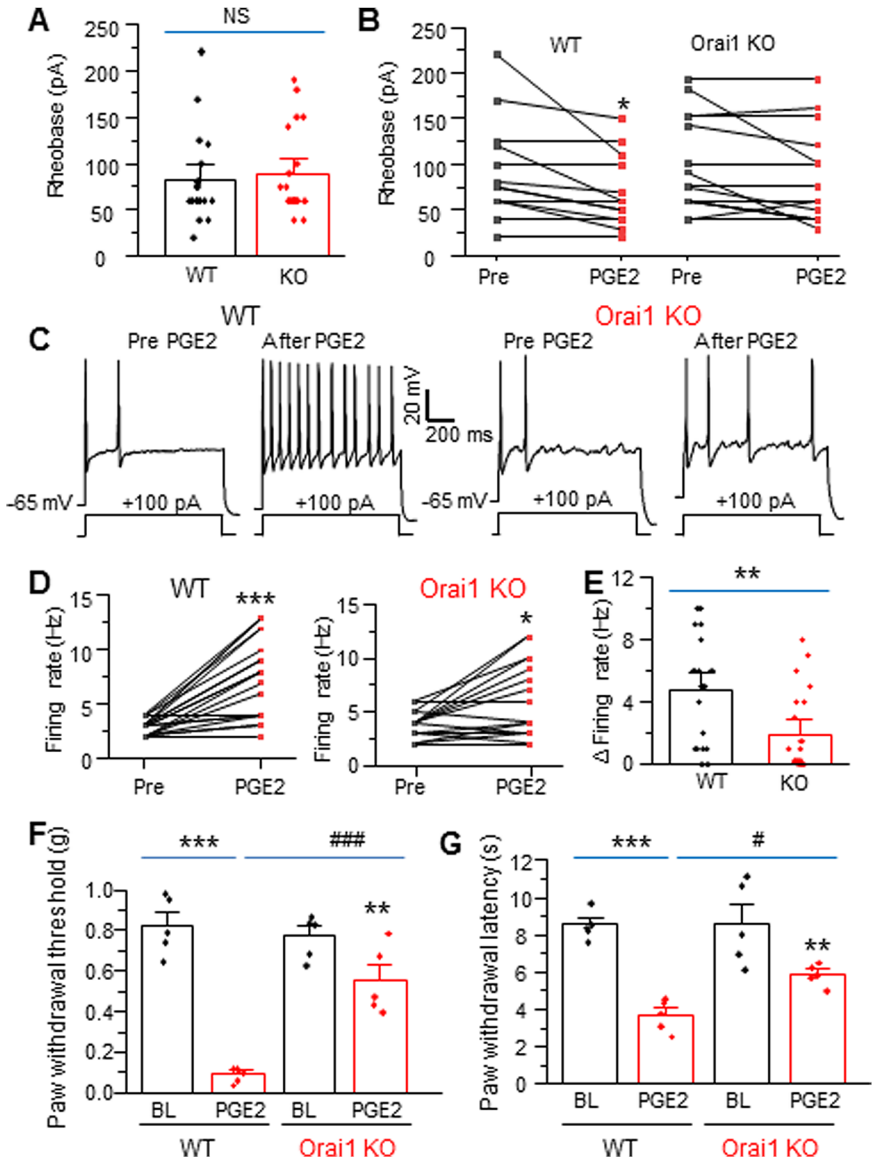

Figure 7. Orai1 contributes to PGE2-induced increase in neuronal excitability and pain hypersensitivity. ***A***, The basal rheobase in WT and Orai1 KO neurons (WT, $n = 19$; Orai1 KO, $n = 20$ from 5 cultures/each genotype). ***B***, Effect of PGE2 on rheobase in WT and Orai1 KO neurons, WT, $n = 19$ neurons; Orai1 KO, $n = 20$ neurons from 5 cultures/each. ***C***, Representative traces of action potential recordings in DRG neurons treated with vehicle (Pre) and PGE2 in WT and Orai1 KO neurons. ***D***, Effect of PGE2 on firing rate in DRG neurons, WT, $n = 20$ neurons; Orai1 KO, $n = 19$ neurons from 5 cultures/each. ***E***, Summary of PGE2-induced changes in the firing rate in WT and Orai1 KO neurons, WT, $n = 20$ neurons; Orai1 KO, $n = 19$ neurons from 5 cultures/each. ***F***, PGE2-induced mechanical hypersensitivity in WT ($n = 5$ mice) and Orai1 KO ($n = 5$ mice) mice. ***G***, PGE2-induced thermal hypersensitivity in WT ($n = 5$ mice) and Orai1 KO ($n = 5$ mice) mice. Values represent mean ± SEM. $^{*}p < 0.05$, $^{**}p < 0.01$, $^{***}p < 0.001$ compared with Orai1 KO by Student's *t* test (***A***, ***E***); compared with Pre by the paired *t* test (***B***, ***D***); or compared with baseline (BL) by one-way ANOVA with Fisher's test (***F***, ***G***). $^{\#}p < 0.05$, $^{\#\#\#}p < 0.001$ compared with WT PGE2 by one-way ANOVA with Fisher's test (***F***, ***G***).

further confirm that the Gq/11-PKC pathway is involved in this process, we also pretreated neurons with a selective inhibitor of Gq/11 protein or PKC before TG-induced Ca^{2+} entry was triggered. Consistently, our results showed that inhibition of Gq/11 or PKC abolished PGE2-mediated SOCE increase in DRG neurons. In contrast, inhibition of PKA had no effect on SOCE. These data suggest that PGE2 potentiates SOC function through the EP1-PKC signaling cascade, rather than the EP4-PKA pathway. It has been shown that ERKs are activated after CFA intraplantar injection (Dai et al., 2004; Obata et al., 2004). PGE2 can induce ERK activation (Cruz Duarte et al., 2012). We therefore examined the involvement of ERKs in this modulation. Our calcium imaging data showed that inhibition of MEK/ERK abolished PGE2-induced SOCE increase. Since inhibition of PKC or ERK completely prevented PGE2-induced increase in SOCE, it is likely that PKC- and ERK-mediated modulation of SOCs via the same pathway. PKC has been shown to activate the ERK cascade in various cell types including neurons (Ueda et al., 1996; Hu et al., 2003; Clark et al., 2004; Dou et al., 2018). We speculate that PGE2 modulates STIM1/Orai1-mediated SOCE through the EP1-PKC-ERK pathway.

Limitations of the study

We have shown that Orai3 also contributes to SOCE in DRG neurons (Wei et al., 2017). The present study showed that deficiency of Orai1 largely reduced SOCE but not completely abolished SOCE, suggesting that Orai3 may mediate the remaining SOCE in DRG neurons. Deletion of Orai3 or combined deletion of both Orai1 and Orai3 would further confirm the contribution of each Orai isoform. Interestingly, we found that PGE2

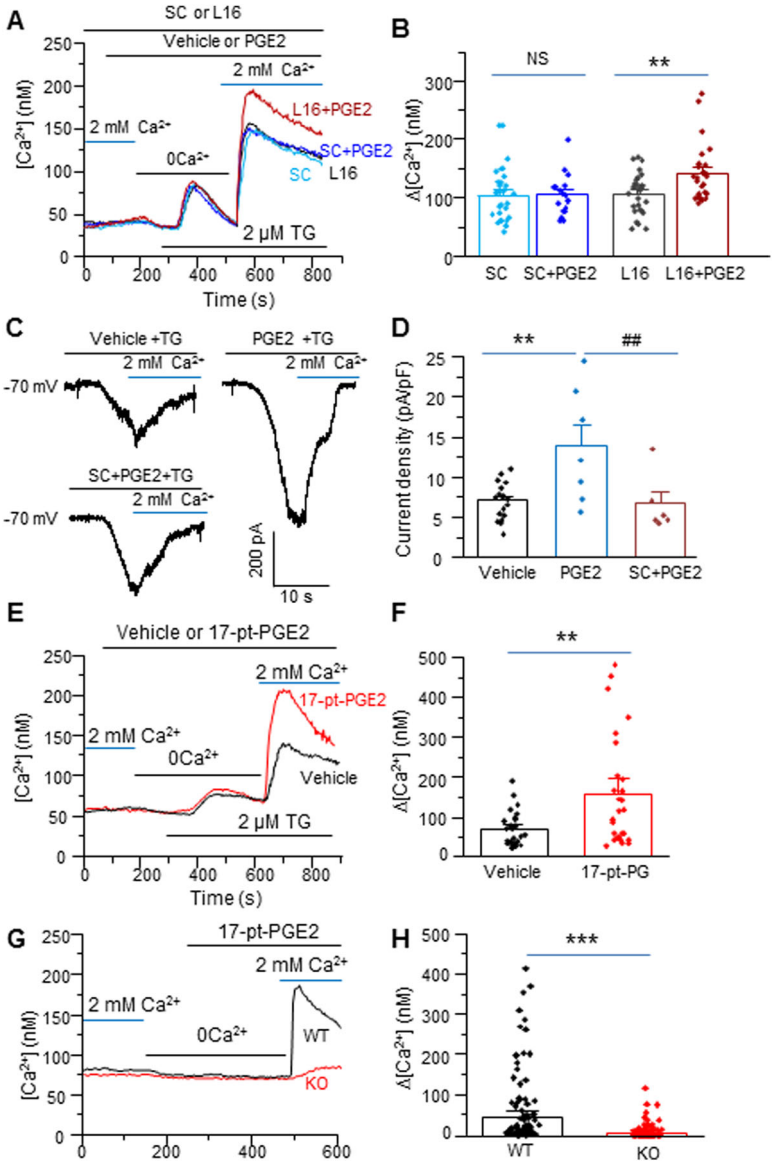

Figure 8. PGE2-induced increase in SOCE is mediated by EP1 in DRG neurons. ***A***, Representative traces of TG-induced SOCE in DRG neurons treated with PGE2 or vehicle in the presence of 20 μM SC19220 (SC) or 1 μM L161982 (L16). ***B***, Effects of SC and L16 on PGE2-induced increase in SOCE, SC, $n = 30$ neurons, SC+PGE2, $n = 17$ neurons, L16, $n = 26$ neurons, L16+PGE2, $n = 26$ neurons from 3 cultures in total. ***C***, Representative recordings of TG-induced SOC currents in DRG neurons pretreated with vehicle or PGE2 in the absence or presence of SC. ***D***, Effect of SC on PGE2-induced increase in SOC currents, PBS, $n = 18$ neurons; PGE2, $n = 7$ neurons; SC+PGE2, $n = 6$ neurons from 7 cultures. ***E***, Representative traces of TG-induced SOCE in DRG neurons treated with vehicle or 17-pt-PGE2. ***F***, Effect of 17-pt-PGE2 on SOCE in DRG neurons, vehicle, $n = 26$ neurons; 17-pt-PGE2, $n = 27$ neurons from two cultures. ***G***, Representative traces of Ca^{2+} removal and addition-induced Ca^{2+} influx in DRG neurons treated with 17-pt-PGE2 in WT and Orai1 KO neurons. ***H***, Effect of 17-pt-PGE2 on Ca^{2+} removal and addition-induced Ca^{2+} influx in DRG neurons cultured from WT and Orai1 KO mice, WT, $n = 125$ neurons; Orai1 KO, $n = 95$ neurons from 2 cultures/each genotype. Values represent mean ± SEM; $^{**}p < 0.01$, $^{***}p < 0.001$ compared with inhibitors or WT by Student's *t* test (***B***, ***F***, ***H***), or compared with vehicle by one-way ANOVA with Tukey's test (***D***). $^{\#\#}p < 0.01$ compared with PGE2 by one-way ANOVA with Tukey's test (***D***). See Extended Data Figures 8-1, 8-2.

selectively regulated Orai1 over Orai3, suggesting an isoform-specific modulation. While Orai1 and Orai3 are highly homologous and share about 60% overall sequence identity (Prakriya and Lewis, 2015), there are several differences in sequence in the N- and C-termini as well as the 2,3 and 3,4 loops (Soboloff et al., 2012). The Orai C-terminus contains Orai-activating region (the major STIM binding area) that differ among the three Orai homologs in their affinity to STIM1 (Frischauf et al., 2009; Park et al., 2009; Tiffner and Derler, 2021). This difference may underlie the isoform-specific modulation. It has been shown that the cytosolic C-terminus domain of STIM1 contains potential multiple ERK phosphorylation sites and ERK activation enhances STIM1 binding to ORAI1, leading to an increase in SOCE (Pozo-Guisado et al., 2010; Lopez-Guerrero et al., 2017). Although our calcium imaging recording did not detect 17-pt-PGE2-induced ER Ca^{2+} release/reduction, indicating that 17-pt-PGE2 may not directly activate STIM1/Orai1, activation of EP1 has been reported to induce ERK activation (Zhang et al., 2007; Cruz Duarte et al., 2012). Our data show that the Ca^{2+}-free solution treatment can slightly increase Ca^{2+} addition-induced Ca^{2+} influx, suggesting some activation of STIM1/Orai1. It is likely that EP1-mediated ERK activation increases STIM1 phosphorylation, subsequently enhancing SOCE. A clear understanding of the isoform-specific modulation of SOCE is still outstanding.

While our in vitro studies show that PGE2-EP1 signaling enhances Orai1-mediated SOCE, how this modulation occurs

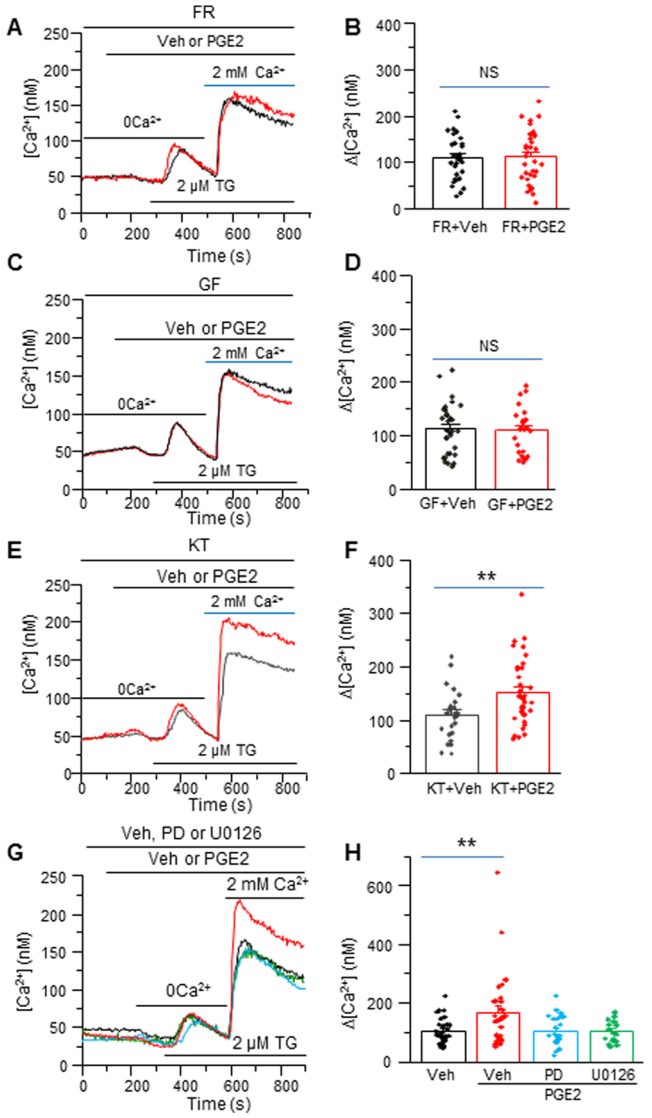

Figure 9. PGE2-induced increase in SOCE is mediated by the Gq-PKC pathway in DRG neurons. ***A***, Representative traces of SOCE in DRG neurons treated with vehicle (Veh) or 1 μM PGE2 in the presence of 100 nM FR900359 (FR). ***B***, Effect of FR on PGE2-induced an increase in SOCE, FR+Veh, $n = 31$ neurons; FR+PGE2, $n = 35$ neurons from 2 cultures. ***C***, Representative traces of SOCE in DRG neurons treated with vehicle or 1 μM PGE2 in the presence of 0.5 μM GF109203X. ***D***, Effect of GF109203X on PGE2-induced an increase in SOCE, GF+Veh, $n = 32$ neurons; GF+PGE2, $n = 25$ neurons from 3 cultures. ***E***, Representative traces of SOCE in DRG neurons treated with vehicle or 1 μM PGE2 in the presence of 1 μM KT5720 alone. ***F***, Effect of KT5720 on PGE2-induced increase in SOCE, KT+Veh, $n = 23$ neurons; KT+PGE2, $n = 38$ neurons from 2 cultures. ***G***, Representative traces of SOCE in DRG neurons treated with vehicle or 1 μM PGE2 in the presence of vehicle, 20 μM PD98059 (PD), and U0126. ***H***, Effects of PD and U0126 on PGE2-induced an increase in SOCE, Vel+PGE2, $n = 30$ neurons, PD+PGE2, $n = 23$ neurons; U0126+PGE2, $n = 16$ neurons from 2 cultures. Values represent mean ± SEM; $^{**}p < 0.01$ compared with inhibitor + Veh by Student's *t* test (***B***, ***D***, ***F***) or one-way ANOVA with Tukey's test (***H***).

in animal models of inflammatory pain remains to be determined. It is known that bradykinin, a primary mediator of pain and inflammation, can induce STIM1 puncta formation and Ca^{2+} entry in rat DRG and trigeminal ganglion neurons (Szteyn et al., 2015; Hogea et al., 2021). Under inflammatory conditions, bradykinin and PGE2 are released/produced in inflamed tissues and mediate pain hypersensitivity (Basbaum et al., 2009). Bradykinin activates SOCs, while PGE2 enhances SOC function, leading to increased neuronal excitability, which may underlie the involvement of Orai1 in peripheral sensitization. Future studies that specifically ablate EP1 in sensory neurons and examine ERK phosphorylation of STIM1 in L3/4 DRGs and SOC function from L3/4 DRG neurons from intraplantar PBS and CFA mice will confirm EP1-ERK-mediated enhancement of SOC function.

In summary, the present study demonstrates that Orai1 plays an important role in peripheral sensitization associated with inflammatory pain. Our data also showed that SOC function is enhanced in DRG neurons under inflammatory conditions. The increased SOCE is induced by inflammatory mediator(s) of PGE2. The modulation of SOCs by PGE2 is likely mediated through the EP1-Gq-PKC-ERK pathway. These findings advance the understanding of the mechanisms underlying PGE2-induced mechanical and thermal hypersensitivity. Enhancing Orai1 function in primary sensory neurons is a novel mechanism underlying PGE2-induced pain hypersensitivity. Our study provides a new insight into the mechanism of inflammatory pain and suggests that targeting Orai1 may represent a new strategy for treating chronic inflammatory pain.

Data availability

The datasets that support the findings of this study are available from the corresponding author upon request.

References

Alfranca A, Iniguez MA, Fresno M, Redondo JM (2006) Prostanoid signal transduction and gene expression in the endothelium: role in cardiovascular diseases. Cardiovasc Res 70:446–456.

Bar KJ, Natura G, Telleria-Diaz A, Teschner P, Vogel R, Vasquez E, Schaible HG, Ebersberger A (2004) Changes in the effect of spinal prostaglandin E2 during inflammation: prostaglandin E (EP1–EP4) receptors in spinal nociceptive processing of input from the normal or inflamed knee joint. J Neurosci 24:642–651.

Basbaum AI, Bautista DM, Scherrer G, Julius D (2009) Cellular and molecular mechanisms of pain. Cell 139:267–284.

Boettger MK, Uceyler N, Zelenka M, Schmitt A, Reif A, Chen Y, Sommer C (2007) Differences in inflammatory pain in nNOS-, iNOS- and eNOS-deficient mice. Eur J Pain 11:810–818.

Brudvik KW, Tasken K (2012) Modulation of T cell immune functions by the prostaglandin E(2)–cAMP pathway in chronic inflammatory states. Br J Pharmacol 166:411–419.

Caselli G, et al. (2018) Pharmacological characterisation of CR6086, a potent prostaglandin E(2) receptor 4 antagonist, as a new potential disease-modifying anti-rheumatic drug. Arthritis Res Ther 20:39.

Clark JA, Black AR, Leontieva OV, Frey MR, Pysz MA, Kunneva L, Woloszynska-Read A, Roy D, Black JD (2004) Involvement of the ERK signaling cascade in protein kinase C-mediated cell cycle arrest in intestinal epithelial cells. J Biol Chem 279:9233–9247.

Clark P, Rowland SE, Denis D, Mathieu MC, Stocco R, Poirier H, Burch J, Han Y, Audoly L, Therien AG, et al. (2008) MF498 [*N*-{[4-(5,9-Diethoxy-6-oxo-6,8-dihydro-7*H*-pyrrolo[3,4-g]quinolin-7-yl)-3-methylbenzyl] sulfonyl}-2-(2-methoxyphenyl)acetamide], a selective E prostanoid receptor 4 antagonist, relieves joint inflammation and pain in rodent models of rheumatoid and osteoarthritis. J Pharmacol Exp Ther 325:425–434.

Crusemann M, et al. (2018) Heterologous expression, biosynthetic studies, and ecological function of the selective Gq-signaling inhibitor FR900359. Angew Chem Int Ed Engl 57:836–840.

Cruz Duarte P, St-Jacques B, Ma W (2012) Prostaglandin E2 contributes to the synthesis of brain-derived neurotrophic factor in primary sensory neuron in ganglion explant cultures and in a neuropathic pain model. Exp Neurol 234:466–481.

Dai Y, Fukuoka T, Wang H, Yamanaka H, Obata K, Tokunaga A, Noguchi K (2004) Contribution of sensitized P2X receptors in inflamed tissue to the mechanical hypersensitivity revealed by phosphorylated ERK in DRG neurons. Pain 108:258–266.

Das UN (2021) Essential fatty acids and their metabolites in the pathobiology of inflammation and its resolution. Biomolecules 11:1873.

DeHaven WI, Smyth JT, Boyles RR, Putney JW Jr. (2007) Calcium inhibition and calcium potentiation of Orai1, Orai2, and Orai3 calcium release-activated calcium channels. J Biol Chem 282:17548–17556.

Dixon WJ (1980) Efficient analysis of experimental observations. Annu Rev Pharmacol Toxicol 20:441–462.

Dou Y, et al. (2018) Orai1 plays a crucial role in central sensitization by modulating neuronal excitability. J Neurosci 38:887–900.

Frischauf I, Muik M, Derler I, Bergsmann J, Fahrner M, Schindl R, Groschner K, Romanin C (2009) Molecular determinants of the coupling between STIM1 and Orai channels: differential activation of Orai1-3 channels by a STIM1 coiled-coil mutant. J Biol Chem 284:21696–21706.

Fuchs A, Lirk P, Stucky C, Abram SE, Hogan QH (2005) Painful nerve injury decreases resting cytosolic calcium concentrations in sensory neurons of rats. Anesthesiology 102:1217–1225.

Ganesh T, Jiang J, Yang MS, Dingledine R (2014) Lead optimization studies of cinnamic amide EP2 antagonists. J Med Chem 57:4173–4184.

Gao R, Gao X, Xia J, Tian Y, Barrett JE, Dai Y, Hu H (2013) Potent analgesic effects of a store-operated calcium channel inhibitor. Pain 154:2034–2044.

Gao XH, Gao R, Tian YZ, McGonigle P, Barrett JE, Dai Y, Hu H (2015) A store-operated calcium channel inhibitor attenuates collagen-induced arthritis. Br J Pharmacol 172:2991–3002.

Gemes G, Bangaru ML, Wu HE, Tang Q, Weihrauch D, Koopmeiners AS, Cruikshank JM, Kwok WM, Hogan QH (2011) Store-operated Ca2+ entry in sensory neurons: functional role and the effect of painful nerve injury. J Neurosci 31:3536–3549.

Gold MS, Reichling DB, Shuster MJ, Levine JD (1996) Hyperalgesic agents increase a tetrodotoxin-resistant Na+ current in nociceptors. Proc Natl Acad Sci U S A 93::1108–1112.

Grynkiewicz G, Poenie M, Tsien RY (1985) A new generation of Ca2+ indicators with greatly improved fluorescence properties. J Biol Chem 260: 3440–3450.

Guay J, Bateman K, Gordon R, Mancini J, Riendeau D (2004) Carrageenan-induced paw edema in rat elicits a predominant prostaglandin E2 (PGE2) response in the central nervous system associated with the induction of microsomal PGE2 synthase-1. J Biol Chem 279:24866–24872.

Hogan PG, Lewis RS, Rao A (2010) Molecular basis of calcium signaling in lymphocytes: STIM and ORAI. Annu Rev Immunol 28:491–533.

Hogea A, Shah S, Jones F, Carver CM, Hao H, Liang C, Huang D, Du X, Gamper N (2021) Junctophilin-4 facilitates inflammatory signalling at plasma membrane-endoplasmic reticulum junctions in sensory neurons. J Physiol 599:2103-2123.

Hu HJ, Gereau RW 4th (2003) ERK integrates PKA and PKC signaling in superficial dorsal horn neurons. II. Modulation of neuronal excitability. J Neurophysiol 90:1680–1688.

Hu HJ, Glauner KS, Gereau RW 4th (2003) ERK integrates PKA and PKC signaling in superficial dorsal horn neurons. I. Modulation of A-type K+ currents. J Neurophysiol 90:1671–1679.

Hu HJ, Carrasquillo Y, Karim F, Jung WE, Nerbonne JM, Schwarz TL, Gereau RW 4th (2006) The kv4.2 potassium channel subunit is required for pain plasticity. Neuron 50:89–100.

Hunter DV, Smaila BD, Lopes DM, Takatoh J, Denk F, Ramer MS (2018) Advillin is expressed in all adult neural crest-derived neurons. eNeuro 5:e0077-18.2018 1–16.

Jang IJ, Davies AJ, Akimoto N, Back SK, Lee PR, Na HS, Furue H, Jung SJ, Kim YH, Oh SB (2017) Acute inflammation reveals GABAA receptor-mediated nociception in mouse dorsal root ganglion neurons via PGE2 receptor 4 signaling. Physiol Rep 5:e13178.

Johansson T, Narumiya S, Zeilhofer HU (2011) Contribution of peripheral versus central EP1 prostaglandin receptors to inflammatory pain. Neurosci Lett 495:98–101.

Kamato D, et al. (2017) Gaq proteins: molecular pharmacology and therapeutic potential. Cell Mol Life Sci 74:1379–1390.

Kassuya CA, Ferreira J, Claudino RF, Calixto JB (2007) Intraplantar PGE2 causes nociceptive behaviour and mechanical allodynia: the role of prostanoid E receptors and protein kinases. Br J Pharmacol 150: 727–737.

Kaufmann U, Shaw PJ, Kozhaya L, Subramanian R, Gaida K, Unutmaz D, McBride HJ, Feske S (2016) Selective ORAI1 inhibition ameliorates autoimmune central nervous system inflammation by suppressing effector but not regulatory T cell function. J Immunol 196:573–585.

Kawabata A (2011) Prostaglandin E2 and pain—an update. Biol Pharm Bull 34:1170–1173.

Konig C, Ebersberger A, Eitner A, Wetzker R, Schaible HG (2022) Prostaglandin EP3 receptor activation is antinociceptive in sensory neurons via PI3Kgamma, AMPK and GRK2. Br J Pharmacol 180:441–458.

Laursen JC, Cairns BE, Dong XD, Kumar U, Somvanshi RK, Arendt-Nielsen L, Gazerani P (2014) Glutamate dysregulation in the trigeminal ganglion: a novel mechanism for peripheral sensitization of the craniofacial region. Neuroscience 256:23–35.

Leclerc JL, Ahmad AS, Singh N, Soshnik-Schierling L, Greene E, Dang A, Dore S (2015) Intracerebral hemorrhage outcomes following selective blockade or stimulation of the PGE2 EP1 receptor. BMC Neurosci 16:48.

Lewis RS (2007) The molecular choreography of a store-operated calcium channel. Nature 446:284–287.

Lim D, Semyanov A, Genazzani A, Verkhratsky A (2021) Calcium signaling in neuroglia. Int Rev Cell Mol Biol 362:1–53.

Lin CR, Amaya F, Barrett L, Wang H, Takada J, Samad TA, Woolf CJ (2006) Prostaglandin E2 receptor EP4 contributes to inflammatory pain hypersensitivity. J Pharmacol Exp Ther 319:1096–1103.

Lopez-Guerrero AM, Pascual-Caro C, Martin-Romero FJ, Pozo-Guisado E (2017) Store-operated calcium entry is dispensable for the activation of ERK1/2 pathway in prostate cancer cells. Cell Signal 40:44–52.

Lopshire JC, Nicol GD (1998) The cAMP transduction cascade mediates the prostaglandin E2 enhancement of the capsaicin-elicited current in rat sensory neurons: whole-cell and single-channel studies. J Neurosci 18:6081–6092.

Ma W (2010) Chronic prostaglandin E2 treatment induces the synthesis of the pain-related peptide substance P and calcitonin gene-related peptide in cultured sensory ganglion explants. J Neurochem 115:363–372.

Ma W, Chabot JG, Vercauteren F, Quirion R (2010) Injured nerve-derived COX2/PGE2 contributes to the maintenance of neuropathic pain in aged rats. Neurobiol Aging 31:1227–1237.

Ma W, St-Jacques B, Rudakou U, Kim YN (2017) Stimulating TRPV1 externalization and synthesis in dorsal root ganglion neurons contributes to PGE2 potentiation of TRPV1 activity and nociceptor sensitization. Eur J Pain 21:575–593.

Matsumoto S, Ikeda M, Yoshida S, Tanimoto T, Takeda M, Nasu M (2005) Prostaglandin E2-induced modification of tetrodotoxin-resistant Na+ currents involves activation of both EP2 and EP4 receptors in neonatal rat nodose ganglion neurones. Br J Pharmacol 145:503–513.

Miller KE, Richards BA, Kriebel RM (2002) Glutamine-, glutamine synthetase-, glutamate dehydrogenase- and pyruvate carboxylase-immunoreactivities in the rat dorsal root ganglion and peripheral nerve. Brain Res 945:202–211.

Minami T, Nakano H, Kobayashi T, Sugimoto Y, Ushikubi F, Ichikawa A, Narumiya S, Ito S (2001) Characterization of EP receptor subtypes responsible for prostaglandin E2-induced pain responses by use of EP1 and EP3 receptor knockout mice. Br J Pharmacol 133:438–444.

Moriyama T, Higashi T, Togashi K, Iida T, Segi E, Sugimoto Y, Tominaga T, Narumiya S, Tominaga M (2005) Sensitization of TRPV1 by EP1 and IP reveals peripheral nociceptive mechanism of prostaglandins. Mol Pain 1:3.

Nakayama Y, Omote K, Kawamata T, Namiki A (2004) Role of prostaglandin receptor subtype EP1 in prostaglandin E2-induced nociceptive transmission in the rat spinal dorsal horn. Brain Res 1010:62–68.

Natura G, et al. (2013) Neuronal prostaglandin E2 receptor subtype EP3 mediates antinociception during inflammation. Proc Natl Acad Sci U S A 110:13648–13653.

Obata K, Yamanaka H, Dai Y, Mizushima T, Fukuoka T, Tokunaga A, Noguchi K (2004) Activation of extracellular signal-regulated protein kinase in the dorsal root ganglion following inflammation near the nerve cell body. Neuroscience 126:1011–1021.

O'Callaghan G, Houston A (2015) Prostaglandin E2 and the EP receptors in malignancy: possible therapeutic targets? Br J Pharmacol 172:5239–5250.

Park CY, Hoover PJ, Mullins FM, Bachhawat P, Covington ED, Raunser S, Walz T, Garcia KC, Dolmetsch RE, Lewis RS (2009) STIM1 clusters and activates CRAC channels via direct binding of a cytosolic domain to Orai1. Cell 136:876–890.

Pozo-Guisado E, Campbell DG, Deak M, Alvarez-Barrientos A, Morrice NA, Alvarez IS, Alessi DR, Martin-Romero FJ (2010) Phosphorylation of STIM1 at ERK1/2 target sites modulates store-operated calcium entry. J Cell Sci 123:3084–3093.

Prakriya M, Lewis RS (2015) Store-operated calcium channels. Physiol Rev 95:1383–1436.

Putney JW (2010) Pharmacology of store-operated calcium channels. Mol Interv 10:209–218.

Putney JW (2011) The physiological function of store-operated calcium entry. Neurochem Res 36:1157–1165.
Qi Z, Wang Y, Zhou H, Liang N, Yang L, Liu L, Zhang W (2016) The central analgesic mechanism of YM-58483 in attenuating neuropathic pain in rats. Cell Mol Neurobiol 36:1035–1043.
Reinold H, et al. (2005) Spinal inflammatory hyperalgesia is mediated by prostaglandin E receptors of the EP2 subtype. J Clin Invest 115:673–679.
Rush AM, Waxman SG (2004) PGE2 increases the tetrodotoxin-resistant Nav1.9 sodium current in mouse DRG neurons via G-proteins. Brain Res 1023:264–271.
Sachs D, Villarreal C, Cunha F, Parada C, Ferreira S (2009) The role of PKA and PKCepsilon pathways in prostaglandin E2-mediated hypernociception. Br J Pharmacol 156:826–834.
Samtleben S, Wachter B, Blum R (2015) Store-operated calcium entry compensates fast ER calcium loss in resting hippocampal neurons. Cell Calcium 58:147–159.
Scholz J, Woolf CJ (2002) Can we conquer pain? Nat Neurosci 5:1062–1067.
Sekiguchi F, Aoki Y, Nakagawa M, Kanaoka D, Nishimoto Y, Tsubota-Matsunami M, Yamanaka R, Yoshida S, Kawabata A (2013) AKAP-dependent sensitization of Ca(v) 3.2 channels via the EP(4) receptor/cAMP pathway mediates PGE(2)-induced mechanical hyperalgesia. Br J Pharmacol 168:734–745.
Shionoya K, Eskilsson A, Blomqvist A (2022) Prostaglandin production selectively in brain endothelial cells is both necessary and sufficient for eliciting fever. Proc Natl Acad Sci U S A 119:e2122562119.
Shu J, Zhang F, Zhang L, Wei W (2017) G protein coupled receptors signaling pathways implicate in inflammatory and immune response of rheumatoid arthritis. Inflamm Res 66:379–387.
Smith JA, Davis CL, Burgess GM (2000) Prostaglandin E2-induced sensitization of bradykinin-evoked responses in rat dorsal root ganglion neurons is mediated by cAMP-dependent protein kinase A. Eur J Neurosci 12:3250–3258.
Soboloff J, Rothberg BS, Madesh M, Gill DL (2012) STIM proteins: dynamic calcium signal transducers. Nat Rev Mol Cell Biol 13:549–565.
Somasundaram A, Shum AK, McBride HJ, Kessler JA, Feske S, Miller RJ, Prakriya M (2014) Store-operated CRAC channels regulate gene expression and proliferation in neural progenitor cells. J Neurosci 34:9107–9123.
Stock JL, et al. (2001) The prostaglandin E2 EP1 receptor mediates pain perception and regulates blood pressure. J Clin Invest 107:325–331.
Szteyn K, Gomez R, Berg KA, Jeske NA (2015) Divergence in endothelin-1- and bradykinin-activated store-operated calcium entry in afferent sensory neurons. ASN Neuro 7:1759091415578714.
Targos B, Baranska J, Pomorski P (2005) Store-operated calcium entry in physiology and pathology of mammalian cells. Acta Biochim Pol 52:397–409.
Theiler A, Konya V, Pasterk L, Maric J, Barnthaler T, Lanz I, Platzer W, Schuligoi R, Heinemann A (2016) The EP1/EP3 receptor agonist 17-pt-PGE(2) acts as an EP4 receptor agonist on endothelial barrier function and in a model of LPS-induced pulmonary inflammation. Vascul Pharmacol 87:180–189.
Tiffner A, Derler I (2021) Isoform-specific properties of Orai homologues in activation, downstream signaling, physiology and pathophysiology. Int J Mol Sci 22:8020.
Ueda Y, Hirai S, Osada S, Suzuki A, Mizuno K, Ohno S (1996) Protein kinase C activates the MEK–ERK pathway in a manner independent of Ras and dependent on Raf. J Biol Chem 271:23512–23519.
Varga DP, Puskas T, Menyhart A, Hertelendy P, Zolei-Szenasi D, Toth R, Ivankovits-Kiss O, Bari F, Farkas E (2016) Contribution of prostanoid signaling to the evolution of spreading depolarization and the associated cerebral blood flow response. Sci Rep 6:31402.
Vasko MR, Habashy Malty R, Guo C, Duarte DB, Zhang Y, Nicol GD (2014) Nerve growth factor mediates a switch in intracellular signaling for PGE2-induced sensitization of sensory neurons from protein kinase A to Epac. PLoS One 9:e104529.
Vig M, DeHaven WI, Bird GS, Billingsley JM, Wang H, Rao PE, Hutchings AB, Jouvin MH, Putney JW, Kinet JP (2008) Defective mast cell effector functions in mice lacking the CRACM1 pore subunit of store-operated calcium release-activated calcium channels. Nat Immunol 9:89–96.
Wang S, Dai Y, Kobayashi K, Zhu W, Kogure Y, Yamanaka H, Wan Y, Zhang W, Noguchi K (2012) Potentiation of the P2X3 ATP receptor by PAR-2 in rat dorsal root ganglia neurons, through protein kinase-dependent mechanisms, contributes to inflammatory pain. Eur J Neurosci 36:2293–2301.
Wei D, Mei Y, Xia J, Hu H (2017) Orai1 and Orai3 mediate store-operated calcium entry contributing to neuronal excitability in dorsal root ganglion neurons. Front Cell Neurosci 11:400.
Woolf CJ, Ma Q (2007) Nociceptors—noxious stimulus detectors. Neuron 55:353–364.
Xia J, Pan R, Gao X, Meucci O, Hu H (2014) Native store-operated calcium channels are functionally expressed in mouse spinal cord dorsal horn neurons and regulate resting calcium homeostasis. J Physiol 592:3443–3461.
Yang D, Gereau RW 4th (2002) Peripheral group II metabotropic glutamate receptors (mGluR2/3) regulate prostaglandin E2-mediated sensitization of capsaicin responses and thermal nociception. J Neurosci 22:6388–6393.
Yang G, Ren Z, Mei YA (2015a) Exposure to 50 Hz magnetic field modulates GABAA currents in cerebellar granule neurons through an EP receptor-mediated PKC pathway. J Cell Mol Med 19:2413–2422.
Yang G, Dong WH, Hu CL, Mei YA (2015b) PGE2 modulates GABAA receptors via an EP1 receptor-mediated signaling pathway. Cell Physiol Biochem 36:1699–1711.
Yang L, Wei Y, Luo Y, Yang Q, Li H, Hu C, Yang Y, Yang J (2017) Effect of PGE2–EPs pathway on primary cultured rat neuron injury caused by aluminum. Oncotarget 8:92004–92017.
Zhang I, Hu H (2020) Store-operated calcium channels in physiological and pathological states of the nervous system. Front Cell Neurosci 14:600758.
Zhang L, Jiang L, Sun Q, Peng T, Lou K, Liu N, Leng J (2007) Prostaglandin E2 enhances mitogen-activated protein kinase/Erk pathway in human cholangiocarcinoma cells: involvement of EP1 receptor, calcium and EGF receptors signaling. Mol Cell Biochem 305:19–26.
Zhou YM, Wu L, Wei S, Jin Y, Liu TT, Qiu CY, Hu WP (2019) Enhancement of acid-sensing ion channel activity by prostaglandin E2 in rat dorsal root ganglion neurons. Brain Res 1724:146442.
Zhu J, et al. (2020) Aberrant subchondral osteoblastic metabolism modifies Na(V)1.8 for osteoarthritis. Elife 9:e57656.
Zurborg S, Piszczek A, Martinez C, Hublitz P, Al Banchaabouchi M, Moreira P, Perlas E, Heppenstall PA (2011) Generation and characterization of an Advillin-Cre driver mouse line. Mol Pain 7:66.